Annual Review of Marine Science

Biogeochemical Controls on Coastal Hypoxia

Katja Fennel[1] and Jeremy M. Testa[2]

[1]Department of Oceanography, Dalhousie University, Halifax, Nova Scotia B3H 4R2, Canada; email: katja.fennel@dal.ca

[2]Chesapeake Biological Laboratory, University of Maryland Center for Environmental Studies, Solomons, Maryland 20688, USA; email: jtesta@umces.edu

Annu. Rev. Mar. Sci. 2019. 11:105–30

First published as a Review in Advance on June 11, 2018

The *Annual Review of Marine Science* is online at marine.annualreviews.org

https://doi.org/10.1146/annurev-marine-010318-095138

Keywords

hypoxia, residence time, estuary, river-dominated shelf, upwelling shelf, anthropogenic nutrient load

Abstract

Aquatic environments experiencing low-oxygen conditions have been described as hypoxic, suboxic, or anoxic zones; oxygen minimum zones; and, in the popular media, the misnomer "dead zones." This review aims to elucidate important aspects underlying oxygen depletion in diverse coastal systems and provides a synthesis of general relationships between hypoxia and its controlling factors. After presenting a generic overview of the first-order processes, we review system-specific characteristics for selected estuaries where adjacent human settlements contribute to high nutrient loads, river-dominated shelves that receive large inputs of fresh water and anthropogenic nutrients, and upwelling regions where a supply of nutrient-rich, low-oxygen waters generates oxygen minimum zones without direct anthropogenic influence. We propose a nondimensional number that relates the hypoxia timescale and water residence time to guide the cross-system comparison. Our analysis reveals the basic principles underlying hypoxia generation in coastal systems and provides a framework for discussing future changes.

1. INTRODUCTION

The phenomenon of low-oxygen conditions in aquatic ecosystems has captured the interest of investigators across the natural sciences for decades. Since the metabolism of all metazoans (multicellular animals) requires oxygen, the phenomenon is of interest to biologists and ecologists. Geochemists are interested because of oxygen's role in reduction–oxidation (redox) reactions that are central in biogeochemical cycles. Physical oceanographers have become increasingly interested in the dynamics of oxygen depletion because it is highly dependent on physical oxygen supply. Hypoxia is a unique research topic given the scales of its temporal and spatial variability, the multitude of its controlling mechanisms, its significance across scientific disciplines, and its increasing societal relevance.

While some aquatic environments are naturally prone to low-oxygen conditions, it has become increasingly clear that anthropogenic nutrient inputs stimulate primary productivity (also referred to as eutrophication) and thus exacerbate oxygen depletion. Links between eutrophication and hypoxia were first recognized in various European and North American lakes in the 1950s and 1960s and were later documented in estuaries, coastal regions, and marginal seas, including Chesapeake Bay, the northern Gulf of Mexico shelf, and the Baltic Sea (Nixon 1998). Anthropogenic nutrient inputs (nutrient loads) result from two main sources: raw or crudely treated wastewater from urban areas, and manure and synthetic fertilizer from agriculture (atmospheric deposition and stormwater runoff also contribute). Because hypoxic conditions negatively affect aquatic organisms and food webs (Vaquer-Sunyer & Duarte 2008), societal commitments have been made to limit the flux of anthropogenic nutrients to fresh, estuarine, and coastal ocean waters.

In this review, we discuss the biogeochemical controls on hypoxia by focusing on selected estuarine and coastal systems around the globe. For these systems, observations and model simulations are available to describe the major underlying processes and long-term changes, enabling a cross-system synthesis. Previous reviews on hypoxia include Diaz & Rosenberg's (2008) seminal contribution linking the global rise of coastal hypoxia to anthropogenic nutrient inputs, Testa & Kemp's (2011) review of biogeochemical drivers and feedbacks, and Breitburg et al.'s (2009) synthesis of the ecological consequences. This review aims to generalize the key aspects of hypoxia development across diverse coastal systems, emphasizing the role that numerical models have played and providing a synthesis of relationships between oxygen depletion and controlling factors.

2. OVERVIEW OF PROCESSES UNDERLYING HYPOXIA GENERATION

The oxygen concentration in a given volume of water is determined by its initial concentration at some arbitrary point in time and the cumulative oxygen sources and sinks that have acted on the volume since that initial time. Oxygen sources include photosynthetic production and any oxygen flux into the volume, e.g., by air–sea gas exchange or physical influx across the volume's perimeter (**Figure 1*a***). Oxygen sinks include biochemical processes, such as respiration by microbes and metazoans; consumption by chemoautotrophs (e.g., nitrifying bacteria); oxidation of reduced chemical species, such as reduced metals and hydrogen sulfide; and export of oxygen by physical transport, uptake by the sediment, and outgassing across the air–sea interface.

Surface waters are well oxygenated because exchange with the atmosphere and photosynthetic production generally exceed the oxygen sinks. In subsurface waters, where photosynthesis is diminished or absent, oxygen sinks dominate, and physical supply is crucial for maintaining well-oxygenated conditions. Hypoxia is generated when oxygen sinks act in combination with restricted supply. The degree of oxygen depletion depends on the magnitude of the net oxygen sink (the sum

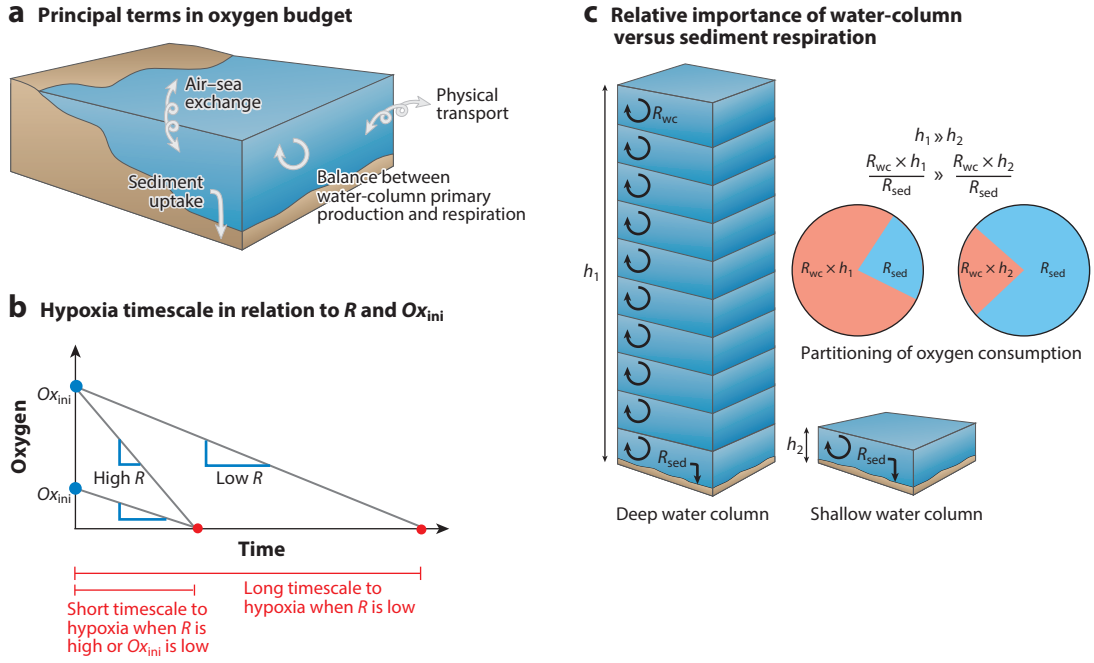

Figure 1

(*a*) Four processes that affect oxygen evolution in a defined control volume: air–sea exchange, sediment uptake, the balance of water-column primary production and respiration, and physical transport across the volume's boundaries. (*b*) Idealized trajectories of oxygen over time in relation to net respiration rate (R) and initial oxygen concentration (Ox_{ini}). (*c*) Schematic contrasting the relative roles of sediment and water-column respiration (R_{sed} and R_{WC}, respectively) in driving total respiration in a deep (h_1) versus shallow (h_2) water column.

of net biochemical consumption in the water column and sediment minus any physical supply) and the duration for which this oxygen sink applies. In other words, hypoxia and ultimately anoxia will occur when sinks exceed sources for long enough to drive oxygen below the hypoxic/anoxic thresholds[1] from its initial concentration (**Figure 1*b***). When biochemical oxygen sinks are large, hypoxia can be generated on short timescales, and relatively short periods of restricted physical oxygen supply will suffice. When biochemical oxygen sinks are small, hypoxia will occur if the physical supply is restricted for sufficiently long.

More formally, we can define the timescale to occurrence of hypoxia, τ_{hyp} (in days), as

$$\tau_{hyp} = \frac{Ox_{ini}}{R},$$

where Ox_{ini} (in mmol O_2 m^{-3}) is the initial oxygen concentration (assumed to be above the hypoxia threshold) and R (in mmol O_2 m^{-3} d^{-1}) is the net oxygen consumption rate. Then the nondimensional number γ, which relates the timescale of hypoxia occurrence to the water residence time τ_{res} (in days),

$$\gamma = \frac{\tau_{hyp}}{\tau_{res}},$$

[1]Hypoxic conditions are generally defined as oxygen concentrations below 2 mg L^{-1} (62.5 mmol O_2 m^{-3}). Anoxic conditions are said to occur when no oxygen is detectable.

must be less than 1 for hypoxia to occur. This number relates the two factors contributing to hypoxia generation—net biochemical oxygen consumption and restricted supply of oxygen, which is related to water residence time.

Net biochemical oxygen consumption is the local rate of consumption minus photosynthetic production. Most photosynthetic production occurs in the surface ocean except in shallow, clear waters, where photosynthesis can occur in and on the sediment because of the presence of benthic algae, submerged rooted macrophytes, and macroalgae. Oxygen consumption occurs through the aerobic respiration of organic matter by microbes and metazoans and the microbial oxidation of reduced inorganic species (e.g., ammonium and hydrogen sulfide). Some of these reduced species are produced during anaerobic microbial respiration of organic matter, which typically occurs in sediments. All oxygen consumption is thus driven by the supply of organic matter regardless of whether its respiration occurs via aerobic or anaerobic pathways. Indeed, a common feature shared by many coastal systems experiencing hypoxia is elevated supply of organic matter, either through direct input from external sources (e.g., sewage) or internal photosynthetic production stimulated by inorganic nutrients, which often stem from anthropogenic sources.

The major nutrients supporting primary production in coastal systems are nitrogen (N) and phosphorus (P). Generally, P is limiting in lakes (i.e., P will be exhausted by primary producers, while an excess of N remains) but N is often limiting in the open ocean. Although coastal systems are typically N limited, P can temporarily be in shorter supply, especially in systems that receive large N inputs. Temporary P limitation is thought to exacerbate hypoxia in some systems (Conley 1999, Paerl et al. 2004) but mitigate hypoxia in others (Laurent & Fennel 2014, 2017). When temporary P limitation occurs, N uptake slows, and the leftover excess N is available later in time and downstream from the P-limited region (**Figure 2**). On the one hand, this can exacerbate hypoxia because a larger region experiences elevated primary production. On the other hand, hypoxia may be diminished because primary production is distributed over a larger area, resulting in lower local rates. These complex spatial and temporal dynamics are difficult to observe directly. Biogeochemical models that realistically simulate coastal circulation and oxygen dynamics have proven useful for elucidating these competing processes.

Oxygen consumption via remineralization of organic matter, regardless of whether it is supplied by external loading or internal production, occurs in the water column and sediments.

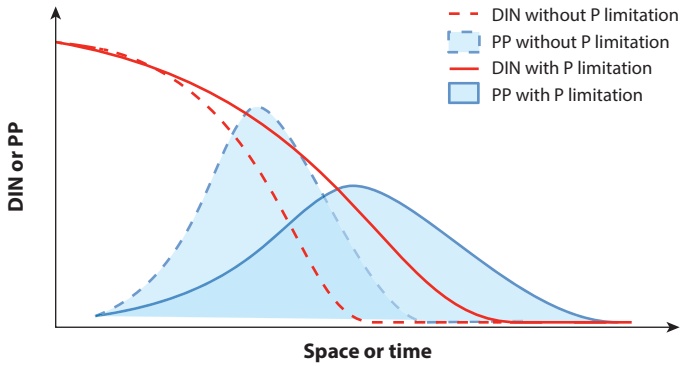

Figure 2

Conceptual model relating the drawdown of dissolved inorganic nitrogen (DIN) concentrations over space or time to primary production (PP). Without phosphorus (P) limitation (*dashed lines*), DIN is consumed earlier and farther upstream, focusing PP in a smaller area with higher peak rates. With P limitation (*solid lines*), DIN is consumed more slowly and farther downstream, supporting a broader area of elevated PP with smaller peak rates.

The relative importance of these two distinct oxygen sinks for hypoxia generation varies by system. The sediment sink generally becomes more important in shallow waters (Kemp et al. 1992, Boynton et al. 2018), partly because shorter water columns provide less space for respiration (**Figure 1*c***) and partly because a larger fraction of sinking labile organic material will reach the sediment. Sediments can act as positive feedback on hypoxia when limited oxygen penetration into sediments diminishes denitrification (Kemp et al. 1990) and stimulates the release of phosphate from ferric complexes (Slomp & Van Cappellen 2007). As a consequence, hypoxia can elevate ammonium and phosphate effluxes from sediments, further stimulating primary production.

Regardless of the biochemical oxygen consumption rate, whether a system develops hypoxia depends on the combination of consumption and physical supply. Coastal hypoxia is often seasonal, occurring during periods of strong density stratification, typically resulting from freshwater inputs, and terminating when vertical mixing erodes density stratification and resupplies oxygen. Exceptions are permanently stratified systems like the Baltic Sea and the Laurentian Channel in the Gulf of St. Lawrence, where permanent stratification prevents vertical mixing of the whole water column. A useful measure for characterizing the degree to which a volume of water is isolated from oxygen supply is residence time, defined as the mean time that water particles are contained within a defined volume. The residence time in coastal systems depends on the bathymetry and circulation regime. Estuaries, which are restricted bathymetrically and characterized by estuarine circulation and strong seasonal stratification, have longer residence times than open shelves. On river-dominated shelves, water residence times are influenced by the magnitude of freshwater input and latitude because the Coriolis force retains fresh water close to the coast except near the equator.

3. OVERVIEW OF COASTAL SYSTEMS EXPERIENCING HYPOXIA

3.1. Estuaries

Estuaries that experience hypoxia include the Baltic Sea, Chesapeake Bay, the Laurentian Channel in the Gulf of St. Lawrence, Long Island Sound, and the Pearl River Estuary (**Figure 3*a*,*b***).

3.1.1. The Baltic Sea. The Baltic Sea is a large, permanently stratified estuary in northern Europe that receives freshwater and nutrient inputs from a large watershed. It has several deep (>200 m), permanently stratified basins with severe hypoxia and anoxia (Carstensen et al. 2014). The large-scale mean circulation comprises a seaward surface flow and a near-bottom inward flow; inflow occurs in sporadic events, on average every 7–10 years, and delivers well-oxygenated, high-salinity water to the deep basins (Matthäus 2006). Thus, hypoxia in this system varies in response to decadal-scale variations in oceanic inflow (Fonselius & Valderrama 2003, Conley et al. 2009) in addition to long-term changes in nutrient inputs. At its maximum extent of approximately 70,000 km^2, the Baltic Sea hypoxic zone is the largest among estuaries and inland seas globally (Carstensen et al. 2014).

Over the past century, the Baltic Sea has received first rising and then decreasing nutrient loads and has warmed by nearly 2°C (Carstensen et al. 2014). While hypoxia was likely present in the Baltic Sea before anthropogenic nutrients loads (Zillén et al. 2008), recent reconstructions suggest that it has expanded over the last century in response to anthropogenic nutrient inputs and elevated respiration due to warming (Jonsson et al. 1990, Carstensen et al. 2014). The intensity and extent of hypoxia in the Baltic Sea allow for measurable changes in bottom-water biogeochemistry. For example, during periods of intense hypoxia, altered biogeochemical processes in deep waters and sediments result in elevated P accumulation (Conley et al. 2002). A long-term expansion of hypoxia is apparent despite its modulation by the sporadic inflows of dense, well-oxygenated waters.

Biogeochemical models have been used to evaluate the relative importance of anthropogenic and natural nutrient inputs and the mechanisms of oxygen supply during the sporadic inflow events, and to project the system's response to projected future changes in temperature and precipitation. Neumann et al. (2002) showed in model scenario simulations that N_2 fixation may increase under reduced nutrient loads, altering the availability and stoichiometry of nutrients in surface waters. Their analysis indicates that hypoxic and anoxic conditions may not respond in an easily predictable manner to reduced nutrient inputs. Neumann et al. (2017) and Meier et al. (2018) have recently carried out detailed model studies of inflow events. These analyses provide alternative explanations for why the third-largest inflow event since 1880, which occurred in late 2014, resulted only in a brief aeration of deep waters and was comparable in its impact on bottom-water oxygen to the much weaker inflow event of 2003. Neumann et al. (2017) suggested that the weak 2003 and the strong 2014 inflow events had a similar impact on bottom-water oxygen conditions because the 2003 event was accompanied by several minor inflow events that resulted in a similar supply of oxygen as in 2014. Meier et al. (2018) emphasized instead an increase in the rate of water-column oxygen consumption in recent years. While the rate of oxygen consumption at depth is relatively low, water-column respiration is the dominant contributor to total respiration in the basins. Meier et al. (2018) suggested that an increase in the rate of water-column oxygen consumption

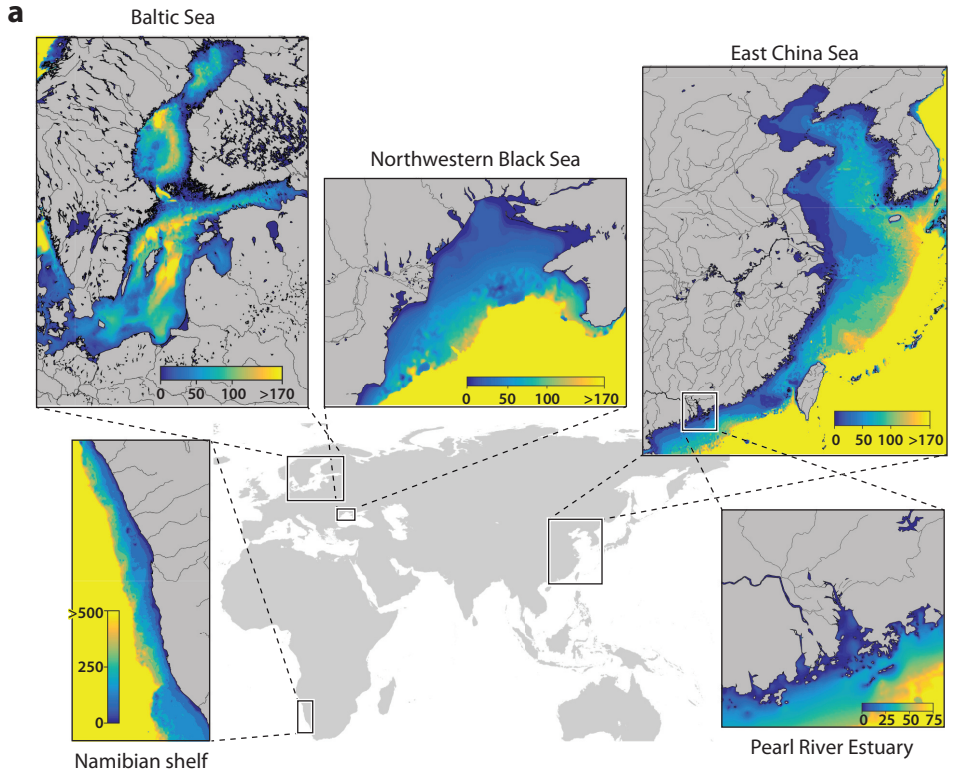

Figure 3

(*a*) Bathymetry of selected coastal systems: the Baltic Sea, the northwestern Black Sea, the East China Sea, the Namibian shelf, and the Pearl River Estuary. (*b*, *next page*) Bathymetry of selected coastal systems: the Oregon shelf, the northern Gulf of Mexico, Chesapeake Bay, the Gulf of St. Lawrence along with the Scotian shelf and Gulf of Maine, and Long Island Sound. The color shows depth (in meters).

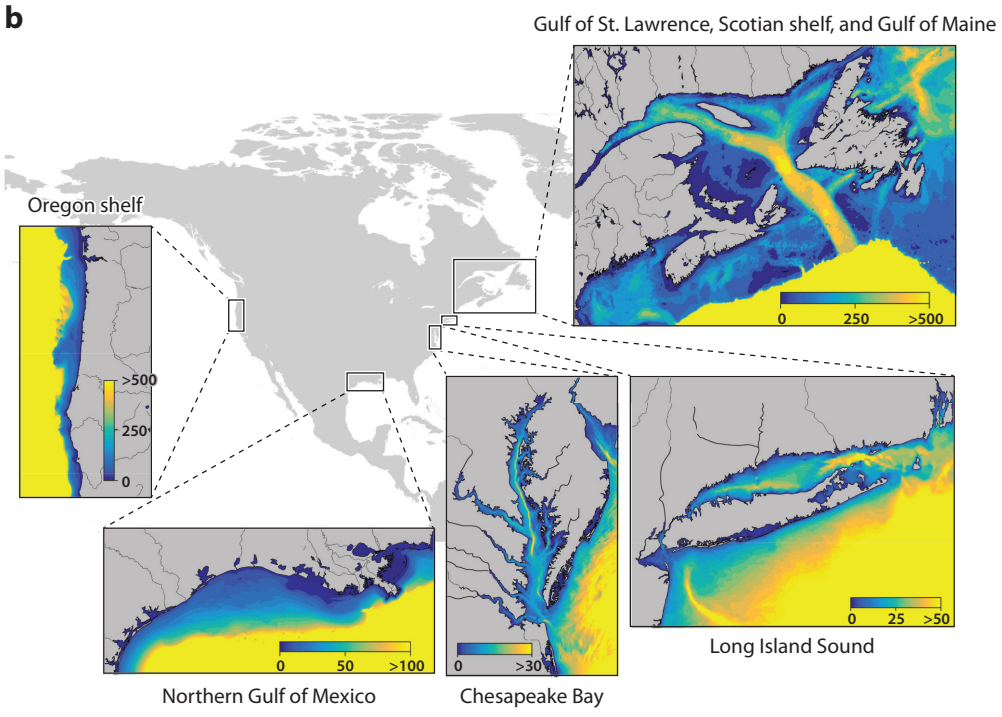

Figure 3

(*Continued*)

has occurred, while sediment consumption has remained unchanged. Model scenarios of future conditions indicate that temperature and precipitation are likely to increase, causing reduced salinity and further reduced oxygen concentrations (Meier et al. 2012).

3.1.2. Chesapeake Bay. Chesapeake Bay receives fresh water, nutrients, and organic matter from several rivers, the largest of which is the Susquehanna. Hypoxia has been documented throughout the past century in Chesapeake Bay and its tributaries (Sale & Skinner 1917) and likely has occurred since the European colonization of eastern North America (Zimmerman & Canuel 2000). Increases in the volume of hypoxic water over the past half century are linked to rising nutrient loads (Hagy et al. 2004). Hypoxia is generally limited to waters below the pycnocline along the central deep (>25 m) channel. Chesapeake Bay's estuarine circulation leads to an estimated mean residence time of 180 days (Du & Shen 2016). The resulting high retention of nutrients and organic matter makes the system particularly vulnerable to eutrophication-driven hypoxia.

Observations over the past three decades have revealed intriguing features of temporal and spatial hypoxia dynamics. Hypoxia initiates in late spring (late April and May) in the landward reaches of the bay's deep central basin, where water is isolated by the bay's estuarine circulation (Testa & Kemp 2014), then expands seaward to occupy large regions of the main channel; the degree of expansion is linked to the amount of freshwater and nutrient inputs (Murphy et al. 2011). In the last three decades, the seasonality of hypoxia appears to have changed, starting earlier and declining later in summer, which is thought to result from a combination of altered stratification and changes in the magnitude of the spring bloom (Murphy et al. 2011, Testa et al.

2018). Observations also indicate that seasonal hypoxia can be temporarily interrupted by the passage of strong storms that induce vertical mixing (Testa et al. 2017). Hypoxia can reestablish quickly after these events when respiration rates are high and stratification returns.

A large number of numerical models of varying complexity and structure have been applied to examine oxygen variability in Chesapeake Bay (Irby et al. 2016 and references therein). Hydrodynamic models with simplified oxygen models have revealed that periods of persistent wind direction drive lateral advection of low-oxygen water onto shallow shoals, where mixing and ventilation occur (Scully 2010). These models have also shown that water-column respiration is the dominant oxygen sink (Li et al. 2015) and that hypoxic volume can be simulated well even when neglecting the sediment sink (Scully 2013). Coupled physical–biogeochemical models have shown that hypoxia is sensitive to changes in both N and P loads (Testa et al. 2014, Li et al. 2016) and that projected future temperatures may exacerbate hypoxia via declining oxygen solubility (Irby et al. 2018).

3.1.3. The Gulf of St. Lawrence. The Gulf of St. Lawrence receives fresh water from the St. Lawrence River and is connected to the North Atlantic through Cabot Strait and the Strait of Belle Isle on the northern and southern sides of Newfoundland. In addition to the river—which is the second largest in North America in terms of fresh water—the Gulf of St. Lawrence receives substantial inflows from the open North Atlantic (Gilbert et al. 2005). Hypoxic conditions persist in the 250-m-deep Laurentian Channel, which extends for 1,200 km from the river mouth to the edge of the continental shelf (Gilbert et al. 2005, Lehmann et al. 2009), because of its permanent density stratification (Saucier et al. 2003, Galbraith 2006).

An observed long-term decline of oxygen in the Laurentian Channel has been attributed primarily to changes in the composition of North Atlantic source water that enters the channel at its mouth (Gilbert et al. 2005). Temperature has increased by approximately 1.65°C over the past 80 years, which could also have contributed to the observed oxygen decline of 1 mmol m^{-3} y^{-1} (Gilbert et al. 2010). Lehmann et al. (2009) suggested that benthic respiration is a key driver of oxygen demand in the Laurentian Channel; their calculations indicated that sediment respiration is 64% of total water-column respiration. This ratio contrasts sharply with the other systems considered here and other cross-system comparisons (Kemp et al. 1992, Boynton et al. 2018). Bourgault et al. (2012) have suggested that water-column respiration is 3–4 times that reported by Lehmann et al. (2009), where model simulations indicated that benthic respiration was only 17% of overall oxygen uptake. While this value is consistent with the other systems in **Figure 4*d***, rates of sediment and water-column respiration in the Gulf of St. Lawrence are comparatively low, suggesting that hypoxia ultimately results from long residence times.

3.1.4. Long Island Sound. Long Island Sound is a semienclosed estuarine system connected to the Atlantic via a relatively open eastern boundary. Unlike many classical systems, the estuary does not have a large freshwater source at its landward edge, instead receiving low-salinity water through several small rivers along its perimeter. The tidally averaged flow in the estuary has been described as a typical estuarine circulation, with surface waters flowing outward to the Atlantic and bottom waters flowing inward (Wilson 1976), but there are seasonal and spatial alterations of the magnitude and direction of circulation (Vieira 2000). While freshwater input is comparatively low, seasonal low-oxygen conditions occur consistently in the westernmost section (the Narrows), which receives high nutrient loadings from wastewater discharged by the New York metropolitan area (Parker & O'Reilly 1991). Oxygen depletion also occurs in the western and central basins of Long Island Sound, but not as consistently as in the Narrows (Lee & Lwiza 2008, Wilson et al. 2015).

Most detailed studies of oxygen depletion in Long Island Sound have focused on the Narrows, an area that is 10–20 m deep and well observed. Seasonal oxygen depletion occurs below a weak

but persistent pycnocline. Multiple reports have suggested a long-term decline in oxygen (Parker & O'Reilly 1991, Wilson et al. 2008), with low oxygen concentrations (<3 mg L^{-1}) in the central and western basins and more severe declines in the Narrows since the 1970s and 1980s. Estimates of both water-column and sediment oxygen consumption suggest that water-column uptake is more important than sediment consumption (Welsh & Eller 1991). Multiple investigators have examined aspects of the controls on hypoxia in Long Island Sound, where possible controlling factors for long-term patterns include alterations to temperature stratification (O'Shea & Brosnan 2000), organic matter production associated with phytoplankton (Lee & Lwiza 2008), and wind-induced changes in circulation (Wilson et al. 2015). Like Chesapeake Bay, alterations of the vertical structure of the water column and circulation changes associated with wind stress are important for hypoxia variability. In Long Island Sound, along-sound wind is associated with ventilation of deeper waters and influences interannual variations in hypoxia (O'Donnell et al. 2008; Wilson et al. 2008, 2015). Changes in wind-induced mixing interact with changes in nutrient loading to drive oxygen depletion, as gradual improvements to sewage treatment processes have yet to cause large reductions in hypoxic area.

3.1.5. The Pearl River Estuary. The Pearl River Estuary is a subtropical estuarine system connected to the continental shelf of the northern South China Sea. It is heavily affected by human activities, with several large cities in its watershed and large nutrient inputs (Dai et al. 2006). The estuary receives inputs from three major tributaries and exports water through several large outlets (Dai et al. 2006). The circulation of the estuary is characterized by a two-layer flow during the wet season but dominated by coastal currents during the dry season (Ji et al. 2011). Hypoxia occurs in relatively shallow water in the lower estuary (<20 m) (Cai et al. 2004, Rabouille et al. 2008), when large nutrient and organic matter inputs drive high rates of respiration (Dai et al. 2006), but tends to be intermittent (Zhang & Li 2010). Sediment oxygen uptake is the dominant respiration sink, reaching as high as 86.2% of total oxygen consumption (Zhang & Li 2010). Despite the large oxygen sink, strong physical forces, including tides and lateral advection, act to replenish oxygen and prevent persistent hypoxia (Zhang & Li 2010). Only during periods of strong vertical stratification does hypoxia develop.

3.2. River-Dominated Shelves

River-dominated shelf systems that receive large freshwater and nutrient inputs and experience seasonal hypoxia include the northern Gulf of Mexico, the East China Sea, and the northwestern Black Sea.

3.2.1. The Northern Gulf of Mexico. The northern Gulf of Mexico is heavily influenced by freshwater and nutrient inputs from the Mississippi/Atchafalaya River system, which drains a large fraction of North America, including the Corn Belt in the Midwest, where industrial fertilizers are heavily applied. Recurring bottom-water hypoxia in summer, extending over a shelf area of approximately 15,000 km^2, has been documented since 1985 (Rabalais et al. 2002) and results from the combination of fresh-water-induced stratification and nutrient-stimulated local production. The N load doubled between the 1950s and mid-1980s, coincident with an exponential increase in the use of synthetic N-based fertilizers (Turner & Rabalais 1991), and has not significantly decreased since then.

Modeling studies for the Gulf of Mexico have shown that the sediment oxygen uptake is of disproportionate importance for hypoxia generation, that P limitation is mitigating hypoxia, and that physical oceanographic forcing is strongly modulating the hypoxic extent and duration. An

important characteristic of this system is that low oxygen concentrations are restricted to the bottom boundary layer, a relatively thin, well-mixed layer above the bottom (Wiseman et al. 1997). Remnants of low-oxygen bottom boundary layers that have detached from the bottom are occasionally observed as oxygen minima at mid-depths in the water column (W. Zhang et al. 2015). Hypoxia simulations performed with different circulation models consistently show the upper limit of hypoxic waters coinciding with that of the bottom boundary layer (Fennel et al. 2016). Since the bottom boundary layer is relatively thin (1–4 m), oxygen consumption by sediments is the dominant oxygen sink within the volume that becomes hypoxic (Fennel et al. 2013, Yu et al. 2015b). Given the importance of sediment oxygen consumption, efforts have been made to improve the representation of biogeochemical coupling between the sediment and the overlying water column (Laurent et al. 2016, Moriarty et al. 2018).

The ratio of inorganic N to P in the Mississippi River varies seasonally between 16:1 and 100:1 and is well above the Redfield ratio of 16:1 for most of the year (Laurent et al. 2012). Especially during peak discharge in spring, the N:P ratio is high, suggesting that photosynthetic nutrient uptake will lead to P exhaustion, leaving behind excess N. Observations of nutrient distributions, measurements of phosphatase enzyme activity, and bioassays have shown that primary production is indeed limited by P during spring and summer (Sylvan et al. 2006, 2007). These observations are reproduced well in model simulations (Laurent et al. 2012, Laurent & Fennel 2014), which show that excess N is transported farther downstream and consumed later due to P limitation. This spreads the nutrient-stimulated primary production over a larger region, essentially resulting in a dilution of organic matter loading to the sediments and a decrease in the area affected by hypoxia (Laurent & Fennel 2014). Scenario simulations for a large suite of nutrient load reductions show that the system is approaching N saturation, where primary production and hypoxia are relatively insensitive to small reductions, while more significant load reductions (∼50%) would return the system to a state where primary production and hypoxia would be more responsive to changes in nutrient load (Fennel & Laurent 2018). According to these scenario simulations, simultaneous reduction in N and P loads would be most effective in reducing hypoxia in the northern gulf (Fennel & Laurent 2018).

There is considerable interannual and short-term variability in hypoxic extent in this region. Statistical analyses by Forrest et al. (2011) and Feng et al. (2012) showed that only 24% of interannual variability in the hypoxic area is explained by spring nutrient load, while inclusion of oceanographic predictors such as the duration of upwelling-favorable wind significantly increases the explained variance. In a follow-up biogeochemical modeling study, Feng et al. (2014) showed mechanistically that upwelling spreads the fresh, chlorophyll-rich river plume across a large fraction of the shelf, thus increasing the area affected by increasing vertical stratification and delivery of organic matter. The hypoxic area and duration are also highly sensitive to the magnitude of wind stress (Yu et al. 2015a). Stochastic processes like meso- and submesoscale instabilities along the plume front determine the exact distribution of plume water, and small perturbations to wind or river forcing can therefore have large effects on the simulated plume location (Marta-Almeida et al. 2013) and hypoxia (Mattern et al. 2013).

3.2.2. The East China Sea. A major source of fresh water and nutrients to the East China Sea is the Changjiang River, the largest river in China and third largest in the world in terms of discharge (Liu et al. 2003). Nutrient loads to the river basin have increased by an order of magnitude since the 1960s (Yan et al. 2003, Wang et al. 2015), largely as a result of China's rapid economic development. China's N-based fertilizer use and domestic livestock doubled between the 1980s and 2000s, and the country surpassed the United States and the European Union in synthetic fertilizer use in 2000

(Liu et al. 2013). Hypoxic zones of approximately 15,000 km^2 have frequently been reported since 2000, although the location can vary significantly from year to year (Zhu et al. 2017). Although hypoxic conditions off the Changjiang River Estuary were observed as early as the 1950s, the affected area has grown with increasing nutrient loads (Wang 2009, Zhu et al. 2011).

Hypoxic conditions off the Changjiang River Estuary are controlled by a more complex interplay of hydrographic and biogeochemical factors than those in the Gulf of Mexico. Three main water masses exert their influence: the Changjiang River plume, also referred to as Changjiang Diluted Water; water supplied by a nearshore branch of the Kuroshio Current, which bifurcates from the main stem at the shelf break northeast of Taiwan and upwells northward into the East China Sea; and water supplied by the Taiwan Warm Current, which flows northward between Taiwan and the Chinese mainland and continues above the nearshore Kuroshio branch (Yang et al. 2011, 2012; Wang et al. 2012; Chi et al. 2017). Onshore transport of Kuroshio water is of the same order of magnitude as the transport through the Taiwan Strait by the Taiwan Warm Current (Guo et al. 2006). The Taiwan Warm Current inflow, with its higher salinity and lower temperature than the Changjiang Diluted Water, is thought to contribute to vertical density stratification in the region affected by hypoxia and supplies bottom water low in oxygen (Wang 2009, Wang et al. 2012). Some have suggested that Taiwan Warm Current water is only a minor contribution to the hypoxic region and emphasized the contribution of subsurface Kuroshio water, which is already low in oxygen when it bifurcates from the main stem and experiences further oxygen drawdown along its path (Qian et al. 2017). The interactions of these different water masses and their responses to variations in wind forcing and river discharge result in significant interannual and short-term variations in the location and severity of hypoxia.

Nevertheless, two distinct low-oxygen regions, one north and one south of 30°N, are often observed and appear to be controlled by a different combination of processes. In the northern region, stratification is strongly influenced by Changjiang Diluted Water, resulting in a sharp, near-surface pycnocline (Chi et al. 2017). In the southern region, the vertical density gradient is broader and larger overall, and low-oxygen conditions are less severe but more persistent (Zhu et al. 2011; Chi et al. 2017). The cool, high-salinity bottom water observed in the southern region is indicative of Kuroshio water, which provides a remote source of nutrients that fuel organic matter production (Chi et al. 2017). While the Changjiang River is a major source of nutrients, supply from open-ocean sources via the Kuroshio and Taiwan Warm Currents is important (Chen & Wang 1999).

Models have proven useful in elucidating the hydrographic complexity of the region (Guo et al. 2006; Yang et al. 2011, 2012) and the relative influence of riverine versus remote nutrients and low-oxygen waters on hypoxia generation. Box model calculations (Chen & Wang 1999) suggested that subsurface Kuroshio water is a more important nutrient source to the East China Sea shelf than inputs from rivers. Simulations with a coupled physical–biological model confirmed that the nearshore Kuroshio branch is a major source of remote nutrients, which intrude along the bottom and are mixed throughout the water column on the shelf during winter (Zhao & Guo 2011). Using a biogeochemical model with dissolved oxygen, Zhou et al. (2017) examined the sensitivity of hypoxic extent to riverine versus offshore nutrient contributions and confirmed sensitivity to both, although simulations with altered river inputs showed a small effect on hypoxia. By contrast, in the Gulf of Mexico, offshore nutrients have a negligible effect on hypoxia (Mattern et al. 2013). In a scenario with increased freshwater discharge and nutrient load from the Changjiang River, only a small effect on hypoxic area was simulated (Zhou et al. 2017), suggesting that riverine nutrients are not the only determinant of hypoxic extent.

Similarly to the Gulf of Mexico, sediment oxygen consumption appears to contribute to hypoxia in the East China Sea. The baseline formulation of the model of Zhou et al. (2017) only considered water-column respiration, neglecting sediment oxygen consumption. When adding the sediment

oxygen sink, Zhou et al. (2017) found a doubling of the simulated hypoxic area, in better agreement with observations. Zhang et al. (2017) measured a mean sediment consumption rate of 23 ± 16 mmol O_2 m^{-2} d^{-1} in the East China Sea, which is similar to rates compiled for the Gulf of Mexico (Yu et al. 2015b) and close to the median of 20 mmol O_2 m^{-2} d^{-1} from a global compilation (Fennel et al. 2009).

Another similarity to the northern Gulf of Mexico is that the river plume is characterized by excess N relative to P, indicating P limitation. Wong et al. (1998) reported excess nitrate (up to 6 mmol N m^{-3}, versus 0.07 mmol P m^{-3}) in surface waters with salinities less than 30.5 covering one-third to half of the East China Sea in 1992. P limitation of phytoplankton growth has also been confirmed experimentally in estuarine and coastal waters in the East China Sea (Harrison et al. 1990). Using a biogeochemical model that includes nitrate and phosphate, Fan & Song (2014) simulated widespread P limitation, as had been postulated by Wong et al. (1998).

3.2.3. The northwestern Black Sea. The shelf in the northwestern Black Sea receives inputs from the Danube, Dniester, and Dnieper Rivers. The Danube and Dnieper are the second- and third-largest rivers in Europe, with the Danube accounting for approximately half of the total freshwater discharge into the Black Sea (Ludwig et al. 2009). The average nutrient concentrations in these rivers were 180 mmol NO_3 m^{-3} and 2.1 mmol PO_4 m^{-3} in the 1990s but dropped by approximately half between the late 1990s and early 2000s, coincident with the breakup of the Soviet Union and Eastern Bloc (Ludwig et al. 2009). Regular monitoring of the northwestern Black Sea during the 1980s and early 1990s documented recurring hypoxia in summer covering an area extending from 10,000 to 20,000 km^2 (Capet et al. 2013 and references therein) and, by one account, exceeding 30,000 km^2 in two years (Mee 2006).

Capet et al. (2013, 2016) used a biogeochemical model to study hypoxia on the northwestern Black Sea shelf. A regression analysis of their multiyear simulation showed that the river nutrient load and the reservoir of labile organic matter in the sediment explains 36% of the simulated variance in hypoxic area (Capet et al. 2013). They also indicated that approximately one-third of organic matter respiration occurs in the sediments, similarly to the northern Gulf of Mexico (Yu et al. 2015b). Also similar to the Gulf of Mexico and the East China Sea is that the duration and spatial extent of enhanced density stratification vary from year to year and are important in determining the spatial extent and duration of hypoxia. This system exemplifies how temporal fluctuations and spatial heterogeneity in hypoxic conditions complicate monitoring: Different data sets have led to drastically different conclusions about the evolution of hypoxia. While Mee (2006) reported a remarkable recovery in the 1990s, coincident with the economic decline of the former Soviet Union, Capet et al.'s (2013) model suggests that no recovery occurred and that insufficient coverage of observations after the mid-1990s has led to misleading conclusions.

3.3. Upwelling Shelves

In the California and Benguela Current systems, upwelling of nutrient-rich, low-oxygen waters driven by equatorward trade winds results in high rates of primary production (Carr 2002, Chavez & Messié 2009). Both systems are associated with oxygen minimum zones generated without direct anthropogenic influence.

3.3.1. The Namibian shelf. The Namibian shelf in the northern Benguela upwelling system, which is highly productive due to near-constant upwelling of nutrient-rich water, regularly experiences hypoxia in its deep, permanently stratified shelf waters inshore of the 200-m isobath. Anoxic conditions with an accumulation of methane and hydrogen sulfide from anaerobic decomposition

of organic matter occasionally occur (Emeis et al. 2004, Lavik et al. 2009). The two main upwelling centers, where wind stress curl is high and the shelf particularly narrow, are located at Cape Frio (18.4°S) and Lüderitz (26.6°S) (Monteiro et al. 2006). Open-ocean subthermocline waters with distinct properties are supplied to the shelf at these two locations: relatively fresh and well-aerated subtropical waters at Lüderitz that ventilate the shelf system, and more saline, nutrient-rich, and hypoxic waters from the Angola gyre at Cape Frio (Mohrholz et al. 2008). This equatorial source water is important for nutrient supply to the shelf but also preconditions shelf waters with low oxygen.

Time-series observations show a clear seasonal cycle of subsurface oxygen, with the lowest concentrations (frequently reaching anoxia) occurring between February and July and oxygen concentrations just above the hypoxic threshold occurring in November and December (Monteiro et al. 2006, 2008). The seasonal oxygen drawdown is out of phase with local respiration, which peaks in October and November, when subsurface oxygen concentrations increase (Monteiro et al. 2006). Although local oxygen consumption contributes to shaping the seasonal cycle, it is driven primarily by the along-shelf transport of the two distinct source waters. Equatorial low-oxygen water, which has its most poleward extension in February, is displaced by better-oxygenated subtropical water from the Lüderitz upwelling center in November, when oxygen is at its peak (Monteiro et al. 2006, 2008; Mohrholz et al. 2008).

Two biogeochemical modeling studies of this region were conducted by Gutknecht et al. (2013) and Schmidt & Eggert (2016). Gutknecht et al. (2013) focused primarily on N cycling processes. In their model, hypoxic conditions offshore of the 300-m isobath are driven by a supply of low-oxygen equatorial water, consistent with the observations, but inshore of the 300-m isobath, hypoxia is generated primarily by local consumption. The latter is in contrast to the observations of Monteiro et al. (2006, 2008) and Mohrholz et al. (2008). Gutknecht et al.'s (2013) model also simulates higher-than-observed minimum oxygen and nitrate concentrations in subsurface waters on the Namibian shelf. The model by Schmidt & Eggert (2016) more realistically reproduces the different source waters and their influence on hypoxia/anoxia and is better able to reproduce subsurface oxygen and nitrate concentrations. Two major differences between the two biogeochemical models are that Schmidt & Eggert (2016) explicitly considered the impact of vertically migrating zooplankton on oxygen and the activity of sulfur-oxidizing bacterial mats on the sediment, which diminish the release of hydrogen sulfide from the sediment under anoxic conditions. However, it is unclear, perhaps even unlikely, that these differences can explain the contrasting oxygen concentrations in the two models, because physical drivers seem to be most important in this system.

Schmidt & Eggert (2016) provided a model-based estimate of water residence time of 40 days for the volume affected by hypoxia (18–23°S, bottom to 400-m depth). In this model, local oxygen consumption is approximately 0.26 mmol m^{-3} d^{-1} in the volume experiencing hypoxia/anoxia, which agrees with available observations. Hence, for well-oxygenated source waters, it would take 1.5–2 years for hypoxic conditions to be reached, well above the estimated water residence time of 40 days. This back-of-the-envelope calculation illustrates that the system would not reach hypoxic or anoxic conditions if source waters were not already low in oxygen. Here, seasonal, interannual, and decadal variations in the severity of hypoxia result primarily from variability in advective oxygen supply (Monteiro et al. 2006, 2008).

3.3.2. The Oregon shelf. The California Current system, which extends along the western margin of North America from Vancouver Island in the north to Baja California in the south, includes the sluggish equatorward eastern limb of the North Pacific gyre, referred to as the California Current; superimposed wind-driven equatorward jets on the shelf; and the subsurface, poleward California Undercurrent (Hickey 1998). On the Oregon shelf, winds tend to be from

the south and downwelling favorable in winter, shifting to upwelling-favorable directions in the spring; this tilts isopycnals upward, supplying nutrient-rich, oxygen-poor waters to the shelf from May to October (Huyer 1983).

The seasonal upwelling preconditions the shelf with low-oxygen water and stimulates primary production, but the local oxygen drawdown does not necessarily reach hypoxic levels. The source water upwelled onto the shelf originates from 100–200-m depth in the slope region, well above the deep-water oxygen minimum zone centered around 700–900-m depth (Grantham et al. 2004). Prior to 2002, hypoxia had not been observed on the Oregon shelf (Grantham et al. 2004, Chan et al. 2008). Since then, oxygen concentrations in the source water have declined, and hypoxic and anoxic events have been occurring frequently (Grantham et al. 2004, Chan et al. 2008). The first occurrence of widespread inner-shelf hypoxia (inside of the 70-m isobath, covering at least 820 km^2) observed in 2002 was attributed to an anomalous invasion of low-oxygen subarctic water into the California Current system (Freeland et al. 2003, Grantham et al. 2004). There is also evidence that upwelling-favorable winds have increased in recent decades, potentially drawing on deeper source waters (García-Reyes et al. 2015).

A physical–biogeochemical model of the California Current system region (Siedlecki et al. 2015) attributes 50–60% of the seasonal oxygen decline on the shelf to respiration, but with some geographic differences. Siedlecki et al. (2015) suggested that the supply of low-oxygen source water and local respiration contribute approximately equally to oxygen drawdown on the Washington shelf but that local respiration is more important on the Oregon shelf.

4. CROSS-SYSTEM PATTERNS OF NUTRIENT INPUTS AND OXYGEN CONSUMPTION

For eight of the estuaries and river-dominated shelves discussed above, we compiled estimates of the thickness of the hypoxic layer and its spatial extent, watershed area, freshwater and nutrient inputs, residence time for the hypoxic volume, and rates of oxygen consumption in the water column and sediment (**Table 1**). We also derived the fraction of oxygen consumption due to sediment uptake in the volume affected by hypoxia and the hypoxia timescale (τ_{hyp}), as defined in Section 2. The comparison reveals basic principles underlying hypoxia generation in coastal systems.

Generally, larger hypoxic areas are related to larger nutrient loads (**Figure 4*a***), indicating that anthropogenic nutrients are an important contributor to hypoxia formation in systems with large freshwater inputs. The Gulf of St. Lawrence and the Baltic Sea deviate from the trend that is indicated by the other systems in **Figure 4*a***. The comparatively modest spatial extent in the Gulf of St. Lawrence is explained by the fact that hypoxia occurs only in the restricted Laurentian Channel (**Figure 3*b***), with a long residence time. In this system, anthropogenic nutrients are considered a minor contributor to hypoxia. Local respiration is low, but the ventilation timescale is long and the source water is low in oxygen (Gilbert et al. 2005). The Baltic Sea has a large hypoxic area compared with the seasonally mixed, river-dominated shelf systems (the East China Sea, northwestern Black Sea, and northern Gulf of Mexico in **Figure 4*a***) because its permanent density stratification prevents seasonal mixing, resulting in slow ventilation.

The wide, passive-margin shelf systems prone to hypoxia (the East China Sea, northwestern Black Sea, and northern Gulf of Mexico) are dominated by rivers that drain intensively farmed watersheds, resulting in high nutrient loads (**Table 1**). An important consideration is whether riverine loads are efficiently exported to the open ocean across the shelf break, transported in the along-shelf direction, or retained near the river mouth. In an idealized numerical analysis of global patterns, Izett & Fennel (2018a,b) showed that for discharges typical of the systems discussed here,

Table 1 Cross-system comparison of selected estuaries and river-dominated shelves

System	Hypoxic-layer thickness (m)	Maximum hypoxic area (mean) (km^2)	Watershed area (km^2)	Discharge ($m^3\ s^{-1}$)	N load (10^6 mol d^{-1})	P load (10^6 mol d^{-1})	Residence time (τ_{res}) (d)	Water-column oxygen consumption (mmol O_2 m^{-3} d^{-1})	Sediment oxygen consumption (mmol O_2 m^{-2} d^{-1})	Sediment fraction of total consumption (%)	Hypoxia timescale (τ_{hyp}) (d)
Estuaries											
Chesapeake Bay	15[a]	1,100[b]	170,000[a]	1,100[c]	17[c]	0.39[c]	180[d]	11[e]	20[f]	11	19
Pearl River	3[g]	ND	450,000[h]	10,000[i]	77[h]	0.82[h]	4[h]	35[j]	66[j]	33	4
Baltic Sea	125[k]	70,000[l] (49,000)	1,700,000[m]	14,000[n]	190[o]	4.1[o]	3,100[k]	0.3[p]	8[q]	17	600
Long Island Sound	12[r]	550[s]	44,000[t]	670[u]	29[v]	0.99[v]	75[w]	9.6[r]	19[r]	8	20
Gulf of St. Lawrence	100[x]	1,300[y]	1,600,000[z]	15,000[α]	130[β]	1.7[β]	730[γ]	0.05[x]	9.7[x]	64	1,500
River-dominated shelves											
Northern Gulf of Mexico	4[δ]	23,000[δ] (15,000)	3,200,000[z]	17,000[ε]	190[h]	3.6[h]	30[ζ]	10.0[η]	20[θ]	33	15
East China Sea	25[κ]	12,000[κ]	1,800,000[h]	29,000[λ]	93[μ]	1.4[μ]	11[h]	28[λ]	23[ξ]	3	8
Northwestern Black Sea	9[π]	20,000[ρ] (15,000)	1,400,000[σ]	8,900[σ]	140[σ]	1.6[σ]	150[ρ]	1.8[φ]	6.8[ρ,χ]	30	89

The characteristics of each system are compiled from the literature sources cited in the footnotes below. For the calculation of the fraction of oxygen consumption by the sediment, the total oxygen consumption is the sum of water-column consumption integrated over the hypoxic layer and sediment oxygen consumption. The definition of the hypoxia timescale is given in Section 2; for this calculation, we used an initial oxygen concentration of 225 mmol O_2 m^{-3}. Abbreviations: N, nitrogen; ND, no data; P, phosphorus.

[a]Kemp et al. 2005; [b]Testa et al. 2014; [c]Q. Zhang et al. 2015; [d]Du & Shen 2016; [e]Smith & Kemp 1995; [f]Boynton et al. 2018; [g]Yin et al. 2004; [h]Rabouille et al. 2008; [i]Cai et al. 2004; [j]Zhang & Li 2010 (modeled); [k]Wulff & Stigebrandt 1989; [l]Carstensen et al. 2014; [m]Wulff et al. 2014; [n]Johansson 2018; [o]Nausch et al. 1999; [p]Pers & Rahm 2000; [q]Noffke et al. 2016; [r]Welsh & Eller 1991; [s]US Environ. Prot. Agency 2017; [t]Wolfe et al. 1991; [u]Gay et al. 2004; [v]J. O'Donnell, unpublished data; [w]Bricker et al. 2007; [x]Lehmann et al. 2009; [y]Belley et al. 2010; [z]Howarth et al. 1996; [α]Saucier & Chasse 2000; [β]Howarth et al. 1996; [γ]Bourgault et al. 2012; [δ]Fennel et al. 2016; [ε]Natl. Park Serv. 2017; [ζ]K. Fennel, unpublished data; [η]Murrell et al. 2013; [θ]Yu et al. 2015b; [κ]Chen et al. 2007; [λ]Chen et al. 2009; [μ]C.-C. Chen, unpublished data; [ξ]Zhou et al. 2017; [π]Cannaby et al. 2015; [ρ]Capet et al. 2013; [σ]Ludwig et al. 2009 (estimated for the Danube, Dnieper, and Dniester); [φ]A. Capet, unpublished data; [χ]Capet et al. 2016.

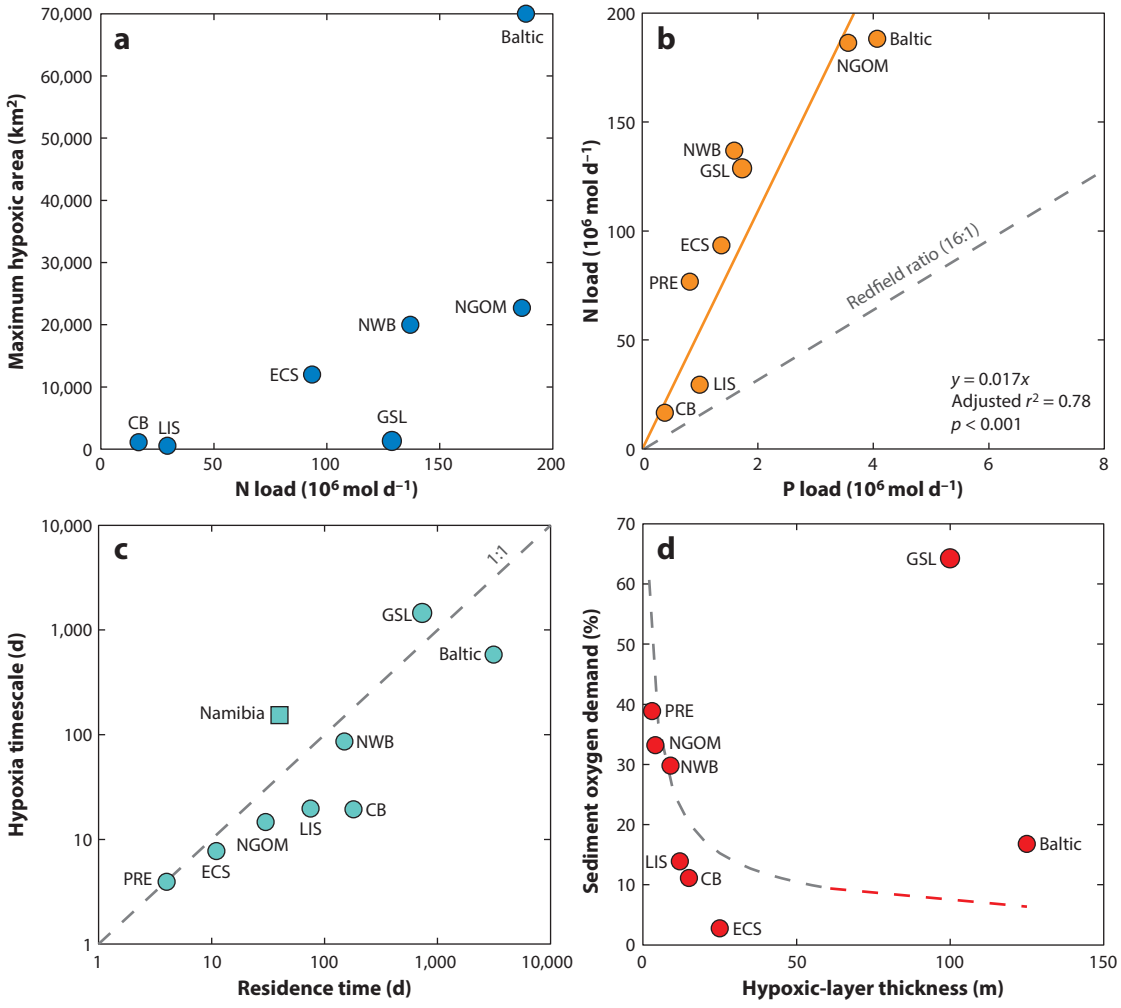

Figure 4

(*a*) Maximum reported hypoxic areas across selected systems plotted over watershed nitrogen (N) load. (*b*) Relationship between N and phosphorus (P) load across systems. The linear fit to the data is indicated by the solid line, and the parameters characterizing the fit are shown at the bottom right. Also indicated is the Redfield ratio of 16:1. (*c*) Hypoxia timescale across systems (including the Namibian shelf, indicated by a *square*; see Section 3.3.1) over residence time. (*d*) Relationship between the percentage of total water-column respiration contributed from sediments and hypoxic-layer thickness. The dashed gray line shows the relationship from Kemp et al. (1992), with the red section indicating an extrapolation to 125-m depth. Abbreviations: CB, Chesapeake Bay; LIS, Long Island Sound; ECS, East China Sea; GSL, Gulf of St. Lawrence; NWB, northwestern Black Sea; NGOM, northern Gulf of Mexico; Baltic, Baltic Sea; PRE, Pearl River Estuary.

20–40% of river source water is locally retained, and cross-shelf export is negligible except for a narrow band along the equator. The Coriolis force deflects the buoyant, nutrient-rich river water into a rotating bulge and downstream current, except in the vicinity of the equator, e.g., for the Amazon River (Sharples et al. 2017). The open-shelf systems discussed here are outside of the equatorial band and thus prone to local retention of fresh water and nutrients.

Nutrient loads tend to be higher in systems with large watersheds, and somewhat surprisingly, the loads of N and P are highly correlated (**Figure 4*b***, **Table 1**). N:P ratios are much larger than

the canonical Redfield ratio of 16:1, indicating a large excess of N. This results in temporary P limitation during and subsequent to discharge peaks, as has been documented for Chesapeake Bay (Fisher et al. 1999), the northern Gulf of Mexico (Sylvan et al. 2006, 2007), and the East China Sea (Wong et al. 1998). As described in Section 2 (see also **Figure 2**), P limitation can exacerbate or mitigate hypoxia, as seen in the northern Gulf of Mexico (Laurent & Fennel 2014).

Rates of oxygen consumption vary widely between systems. In general, water-column respiration tends to be smaller in deeper systems (the Baltic Sea and Gulf of St. Lawrence), where the consumption of sinking organic matter is distributed across a longer water column. Sediment oxygen uptake is also negatively related to depth because a smaller fraction of organic material produced in surface layers reaches the seafloor. Prior cross-system comparisons for estuarine environments have revealed a negative exponential relationship between the fraction of total oxygen consumption due to sediment uptake and depth (Kemp et al. 1992, Boynton et al. 2018). Our compilation generally agrees with this result, although sediments tend to make a smaller contribution to respiration here, and the Gulf of St. Lawrence is an outlier (**Figure 4*d***).

The hypoxia timescale (τ_{hyp}), which indicates how long it will take for a control volume to reach hypoxic conditions from an assumed initial oxygen concentration, varies by three orders of magnitude in our compilation (**Table 1**). The largest estimates, on the order of years, were obtained for the Gulf of St. Lawrence and the Baltic Sea; other systems have hypoxia timescales on the order of days to weeks. As stated in Section 2, even systems with long hypoxia timescales will become hypoxic if the oxygen supply is restricted for sufficiently long. Residence time, a measure of ventilation, is a major factor in determining whether hypoxia occurs. This is illustrated by comparing the large, semienclosed basins with restricted ventilation (the Baltic Sea and Gulf of St. Lawrence) with seasonally mixed estuaries (Chesapeake Bay and Long Island Sound) and the shelf systems summarized in **Table 1**. In fact, the timescale of hypoxia generation is related to residence time (**Figure 4*c***). As predicted in Section 2, the nondimensional number γ, which relates the hypoxia timescale to water residence time, is less than 1 for the majority of systems analyzed here (**Figure 4*c***). The Pearl River Estuary has the lowest hypoxia timescale and lowest residence time in our compilation. The Namibian shelf and Gulf of St. Lawrence are exceptions to this pattern when a large initial concentration is assumed (as we have done for the calculations in **Table 1**), further illustrating the importance of low-oxygen source water to hypoxia generation in these systems. As discussed above, on narrow upwelling shelves, including those off Oregon (Grantham et al. 2004, Chen et al. 2009) and Namibia (Monteiro et al. 2006, 2008), advection of low-oxygen water onto the shelf is an important driver of hypoxia.

5. FUTURE OUTLOOK

There is a rapidly growing body of scientific literature on potential consequences of rising anthropogenic carbon emissions and synthetic fertilizer application for coastal biogeochemistry. Commonly cited prospects include changes to the physical environment (e.g., warming); changes in freshwater inputs (Sinha et al. 2017); changes in the variability and magnitude of wind forcing (García-Reyes et al. 2015); changes in nutrient inputs, especially in developing countries with rapidly growing populations and expanding fertilizer-intensive farming (Seitzinger et al. 2010); and synergies with other stressors, particularly ocean acidification (Cai et al. 2011). Continued warming and acidification are predicted with high confidence. By contrast, the direction and magnitude of changes in precipitation, wind stress, and nutrient loading are uncertain and highly region specific. Contributing further to the challenge of projecting future hypoxia is that many biogeochemical responses are nonlinear and compensatory and involve feedbacks that may amplify or dampen a given interaction.

Perhaps the most widely anticipated feature is warming, which has already been documented in several cases that showed water temperature increases of at least 1°C over the past 30 years (Testa et al. 2018). Warming has the potential to increase the intensity, duration, and spatial extent of hypoxia by increasing stratification, decreasing the solubility of oxygen in seawater, and increasing the rate of organic matter remineralization and thus oxygen consumption. In practice, however, these predictions may be too simplistic. In many coastal regions experiencing hypoxia (e.g., the northern Gulf of Mexico, the East China Sea, and Chesapeake Bay), salinity has a much stronger effect on stratification than temperature does. Indeed, in future projections for the northern Gulf of Mexico, Lehrter et al. (2017) and Laurent et al. (2018) found only modest increases in spatial hypoxic extent but more severe and prolonged exposure to hypoxic conditions in the future. Laurent et al. (2018) showed that the warming-induced expansion is due mostly to a decrease in oxygen solubility and less so to stronger stratification. For Chesapeake Bay, oxygen solubility was also the primary driver of future hypoxia, being more important than increases in salinity and stratification due to sea level rise (Irby et al. 2018). It is also unlikely that temperature will strongly amplify the total annual respiratory oxygen sink that acts on a system. While there is ample evidence that rising temperatures will speed up the respiration of freshly deposited organic matter (Smith & Kemp 1995, Carstensen et al. 2014), ultimately respiration is determined by the amount of organic matter available.

The potential impacts of changes in freshwater input are twofold. Larger discharges would increase stratification, thus amplifying hypoxia, while diluting nutrients (assuming constant load) would likely mitigate hypoxia. Both of these effects were seen in model simulations of Laurent & Fennel (2014) for the northern Gulf of Mexico and Irby et al. (2018) for Chesapeake Bay. On the other hand, precipitation amount, frequency, and intensity in the watershed are major controls on riverine N load (Lee et al. 2016). By combining an empirical model of N loading with Coupled Model Intercomparison Project Phase 5 (CMIP5) climate projections, Sinha et al. (2017) predicted that projected increases in total and extreme precipitation will elevate total N loading in the continental United States by approximately 20% by 2100 in the business-as-usual scenario. Projected increases are especially pronounced for the northeastern United States and upper Mississippi/Atchafalaya River basin, regions with historically high N fluxes. Sinha et al. (2017) also suggested that large portions of East, South, and Southeast Asia, including India and eastern China, have similar risk factors and are therefore likely to experience large precipitation-driven increases in N load.

The other major factor determining N loading from the watershed is N input through farming and other land use practices. Seitzinger et al. (2010) showed that the future trajectory of N loading is highly dependent on socioeconomic drivers. Assuming the Global Orchestration scenario (which includes intensive agriculture and rapid increases in fertilizer use in developing countries) leads to predictions of increasing N loads, while under the Adapting Mosaic scenario (which assumes modest increases in global fertilizer use and moderate improvements in its efficiency), N loads would decrease for many countries. Regardless of the scenario, large changes are expected in South Asia (Seitzinger et al. 2010).

Projections of changes in future wind forcing are highly uncertain but can affect coastal hypoxia in significant ways. In eastern boundary current systems, wind forcing is not only the driver of nutrient supply to the continental shelf but also responsible for onwelling of low-oxygen source waters. This preconditions the Namibian and Oregon shelves to low-oxygen conditions (see Section 3.3). A long-term shift toward more upwelling-favorable winds has been implicated in the recent emergence of hypoxic and anoxic conditions on the Oregon shelf (Grantham et al. 2004, García-Reyes et al. 2015). In Chesapeake Bay and Long Island Sound, observational and modeling studies have shown the importance of both wind speed and direction in influencing the

extent of hypoxia (Wilson et al. 2008; Scully 2010, 2016; Li et al. 2015). Increases in wind strength could decrease hypoxia by eroding vertical stratification and aerating bottom waters, especially in shelf regions without permanent stratification, like the northern Gulf of Mexico (Yu et al. 2015a).

Additional stressors on coastal ecosystems besides oxygen depletion are warming and acidification (i.e., decreasing pH of seawater), the latter of which is intricately linked with low oxygen. Acidification results principally from an accumulation of dissolved inorganic carbon due to two distinct processes: respiration of organic matter and oceanic uptake of atmospheric CO_2. Acidification due to respiration occurs because of the same process that leads to low-oxygen conditions: the accumulation of respiration-derived inorganic carbon without sufficient ventilation. This process can be driven by eutrophication, as in the northern Gulf of Mexico (Cai et al. 2011, Laurent et al. 2017), or by increased upwelling of low-oxygen, carbon-rich source waters, as on the Oregon shelf, where the emergence of hypoxic/anoxic events described in Section 3.3.2 coincides with the occurrence of low-pH conditions on the shelf (Feely et al. 2008). The respiration-driven acidification is increasingly amplified by the ocean's uptake of anthropogenic carbon from the atmosphere. Projections for the northern Gulf of Mexico indicate that, under a business-as-usual scenario, the pH of seasonally hypoxic waters will decrease dramatically due to uptake of atmospheric CO_2, reaching the limit for aragonite saturation by the end of this century (Laurent et al. 2018). In other estuaries and coastal systems (e.g., Chesapeake Bay and the North Sea), pH is also predicted to decline (Blackford & Gilbert 2007, Cai et al. 2017).

The number of projected environmental changes, their potential interactions, and uncertainty in their magnitude and (in some cases) direction make it difficult to predict the future of coastal hypoxia. We can state with confidence that coastal waters will warm and that their pH will decrease. Some regions will likely see increases in freshwater and nutrient inputs, which will almost certainly exacerbate hypoxic conditions, but changes in wind forcing remain a wild card. Numerical models that simulate coupled physical–biogeochemical processes with increasing realism have proven useful in elucidating the mechanistic interplay and relative importance of the different factors contributing to hypoxia generation. They are also our best available tools for projecting into the future.

DISCLOSURE STATEMENT

The authors are not aware of any affiliations, memberships, funding, or financial holdings that might be perceived as affecting the objectivity of this review.

ACKNOWLEDGMENTS

K.F. acknowledges funding from the Natural Sciences and Engineering Research Council of Canada (NSERC) Discovery program. This is University of Maryland Center for Environmental Science (UMCES) contribution number 5491.

LITERATURE CITED

Belley R, Archambault P, Sundby B, Gilbert F, Gagnon J-M. 2010. Effects of hypoxia on benthic macrofauna and bioturbation in the Estuary and Gulf of St. Lawrence, Canada. *Cont. Shelf Res.* 30:1302–13

Blackford JC, Gilbert FJ. 2007. pH variability and CO_2 induced acidification in the North Sea. *J. Mar. Syst.* 64:229–41

Bourgault D, Cyr F, Galbraith PS, Pelletier E. 2012. Relative importance of pelagic and sediment respiration in causing hypoxia in a deep estuary. *J. Geophys. Res. Oceans* 117:C08033

Boynton WR, Ceballos MAC, Bailey EM, Hodgkins CLS, Humphrey JL, Testa JM. 2018. Oxygen and nutrient exchanges at the sediment-water interface: a global synthesis and critique of estuarine and coastal data. *Estuaries Coasts* 41:301–33

Breitburg DL, Hondorp DW, Davias LA, Diaz RJ. 2009. Hypoxia, nitrogen, and fisheries: integrating effects across local and global landscapes. *Annu. Rev. Mar. Sci.* 1:329–49

Bricker S, Longstaff B, Dennison W, Jones A, Boicourt K, et al. 2007. *Effects of nutrient enrichment in the nation's estuaries: a decade of change*. Rep., NOAA Coast. Ocean Program Decis. Anal. Ser. 26, Natl. Cent. Coast. Ocean Sci., Silver Spring, MD

Cai W-J, Dai M, Wang Y, Zhai W, Huang T, et al. 2004. The biogeochemistry of inorganic carbon and nutrients in the Pearl River Estuary and the adjacent northern South China Sea. *Cont. Shelf Res.* 24:1301–19

Cai W-J, Hu X, Huang W-J, Murrell MC, Lehrter JC, et al. 2011. Acidification of subsurface coastal waters enhanced by eutrophication. *Nat. Geosci.* 4:766–70

Cai W-J, Huang W-J, Luther GW III, Pierrot D, Li M, et al. 2017. Redox reactions and weak buffering capacity lead to acidification in the Chesapeake Bay. *Nat. Commun.* 8:369

Cannaby H, Fach BA, Arkin SS, Salihoglu B. 2015. Climatic controls on biophysical interactions in the Black Sea under present day conditions and a potential future (A1B) climate scenario. *J. Mar. Syst.* 141:149–66

Capet A, Beckers J-M, Grégoire M. 2013. Drivers, mechanisms and long-term variability of seasonal hypoxia on the Black Sea northwestern shelf – is there any recovery after eutrophication? *Biogeosciences* 10:3943–62

Capet A, Meysman FJR, Akoumianaki I, Soetaert K, Grégoire M. 2016. Integrating sediment biogeochemistry into 3D oceanic models: a study of benthic-pelagic coupling in the Black Sea. *Ocean Model.* 101:83–100

Carr ME. 2002. Estimation of potential productivity in Eastern Boundary Currents using remote sensing. *Deep-Sea Res. II* 49:59–80

Carstensen J, Andersen JH, Gustafsson BG, Conley DJ. 2014. Deoxygenation of the Baltic Sea during the last century. *PNAS* 111:5628–33

Chan F, Barth JA, Lubchenco J, Kirincich A, Weeks H, et al. 2008. Emergence of anoxia in the California Current large marine ecosystem. *Science* 319:920

Chavez FP, Messié M. 2009. A comparison of Eastern Boundary Upwelling Ecosystems. *Prog. Oceanogr.* 83:80–96

Chen C-C, Gong G-C, Shiah F-K. 2007. Hypoxia in the East China Sea: one of the largest coastal low-oxygen areas in the world. *Mar. Environ. Res.* 64:399–408

Chen C-C, Shiah F-K, Chiang K-P, Gong G-C, Kemp WM. 2009. Effects of the Changjiang (Yangtze) River discharge on planktonic community respiration in the East China Sea. *J. Geophys. Res. Oceans* 114:C03005

Chen C-TA, Wang S-L. 1999. Carbon, alkalinity and nutrient budgets on the East China Sea continental shelf. *J. Geophys. Res. Oceans* 104:20675–86

Chi L, Song X, Yuan Y, Wang W, Zhou P, et al. 2017. Distribution and key influential factors of dissolved oxygen off the Changjiang River Estuary (CRE) and its adjacent waters in China. *Mar. Pollut. Bull.* 125:440–50

Conley DJ. 1999. Biogeochemical nutrient cycles and nutrient management strategies. *Hydrobiologia* 410:87–96

Conley DJ, Björck S, Bonsdorff E, Carstensen J, Destouni G, et al. 2009. Hypoxia-related processes in the Baltic Sea. *Environ. Sci. Technol.* 43:3412–20

Conley DJ, Humborg C, Rahm L, Savchuk OP, Wulff F. 2002. Hypoxia in the Baltic Sea and basin-scale changes in phosphorus biogeochemistry. *Environ. Sci. Technol.* 36:5315–20

Dai M, Guo X, Zhai W, Yuan L, Wang B, et al. 2006. Oxygen depletion in the upper reach of the Pearl River estuary during a winter drought. *Mar. Chem.* 102:159–69

Diaz RJ, Rosenberg R. 2008. Spreading dead zones and consequences for marine ecosystems. *Science* 321:926–29

Du J, Shen J. 2016. Water residence time in Chesapeake Bay for 1980–2012. *J. Mar. Syst.* 164:101–11

Emeis KC, Brüchert V, Currie B, Endler R, Ferdelman T, et al. 2004. Shallow gas in shelf sediments of the Namibian coastal upwelling ecosystem. *Cont. Shelf Res.* 24:627–42

Fan W, Song J. 2014. A numerical study of the seasonal variations of nutrients in the Changjiang River estuary and its adjacent sea area. *Ecol. Model.* 291:69–81

Feely RA, Sabine CL, Hernandez-Ayon JM, Ianson D, Hales B. 2008. Evidence for upwelling of corrosive "acidified" water onto the continental shelf. *Science* 320:1490–92
Feng Y, DiMarco SF, Jackson GA. 2012. Relative role of wind forcing and riverine nutrient input on the extent of hypoxia in the northern Gulf of Mexico. *Geophys. Res. Lett.* 39:L09601
Feng Y, Fennel K, Jackson GA, DiMarco SF, Hetland RD. 2014. A model study of the response of hypoxia to upwelling favorable wind on the northern Gulf of Mexico shelf. *J. Mar. Syst.* 131:63–73
Fennel K, Brady D, DiToro D, Fulweiler R, Gardner WS, et al. 2009. Modelling denitrification in aquatic sediments. *Biogeochemistry* 93:159–78
Fennel K, Hu J, Laurent A, Marta-Almeida M, Hetland R. 2013. Sensitivity of hypoxia predictions for the Northern Gulf of Mexico to sediment oxygen consumption and model nesting. *J. Geophys. Res. Oceans* 118:990–1002
Fennel K, Laurent A. 2018. N and P as ultimate and proximate limiting nutrients in the northern Gulf of Mexico: implications for hypoxia reduction strategies. *Biogeosciences* 15:3121–31
Fennel K, Laurent A, Hetland R, Justić D, Ko DS, et al. 2016. Effects of model physics on hypoxia simulations for the northern Gulf of Mexico: a model intercomparison. *J. Geophys. Res. Oceans* 121:5731–50
Fisher TR, Gustafson AB, Sellner K, Lacouture R, Haas LW, et al. 1999. Spatial and temporal variation of resource limitation in Chesapeake Bay. *Mar. Biol.* 133:763–78
Fonselius S, Valderrama J. 2003. One hundred years of hydrographic measurements in the Baltic Sea. *J. Sea Res.* 49:229–41
Forrest DR, Hetland RD, DiMarco SF. 2011. Multivariable statistical regression models of the areal extent of hypoxia over the Texas–Louisiana continental shelf. *Environ. Res. Lett.* 6:045002
Freeland HJ, Gatien G, Huyer A, Smith RL. 2003. Cold halocline in the northern California current: an invasion of subarctic water. *Geophys. Res. Lett.* 30:1141
Galbraith PS. 2006. Winter water masses in the Gulf of St. Lawrence. *J. Geophys. Res. Oceans* 111:C06022
García-Reyes M, Sydeman WJ, Schoeman DS, Rykaczewski RR, Black BA, et al. 2015. Under pressure: climate change, upwelling, and Eastern Boundary Upwelling Ecosystems. *Front. Mar. Sci.* 2:109
Gay PS, O'Donnell J, Edwards CA. 2004. Exchange between Long Island Sound and adjacent waters. *J. Geophys. Res. Oceans* 109:C06017
Gilbert D, Rabalais N, Díaz R, Zhang J. 2010. Evidence for greater oxygen decline rates in the coastal ocean than in the open ocean. *Biogeosciences* 7:2283–96
Gilbert D, Sundby B, Gobeil C, Mucci A, Tremblay G-H. 2005. A seventy-two year record of diminishing deep-water oxygen in the St. Lawrence estuary: the northwest Atlantic connection. *Limnol. Oceanogr.* 50:1654–66
Grantham BA, Chan F, Nielsen KJ, Fox DS, Barth JA, et al. 2004. Upwelling-driven nearshore hypoxia signals ecosystem and oceanographic changes in the northeast Pacific. *Nature* 429:749–54
Guo X, Miyazawa Y, Yamagata T. 2006. The Kuroshio onshore intrusion along the shelf break of the East China Sea: the origin of the Tsushima Warm Current. *J. Phys. Oceanogr.* 36:2205–31
Gutknecht E, Dadou I, Le Vu B, Cambon G, Sudre J, et al. 2013. Coupled physical/biogeochemical modeling including O_2-dependent processes in the Eastern Boundary Upwelling Systems: application in the Benguela. *Biogeosciences* 10:3559–91
Hagy JD, Boynton WR, Keefe CW, Wood KV. 2004. Hypoxia in Chesapeake Bay, 1950–2001: long-term change in relation to nutrient loading and river flow. *Estuaries* 27:634–58
Harrison PJ, Hu MH, Yang YP, Lu X. 1990. Phosphate limitation in estuarine and coastal waters on China. *J. Exp. Mar. Biol. Ecol.* 140:79–97
Hickey BM. 1998. Coastal oceanography of western North America from the tip of Baja California to Vancouver Island. In *The Sea*, Vol. 11: *The Global Coastal Ocean: Regional Studies and Syntheses*, ed. AR Robinson, KH Brink, pp. 345–93. New York: Wiley & Sons
Howarth RW, Billen G, Swaney D, Townsend A, Jaworski N, et al. 1996. Regional nitrogen budgets and riverine N & P fluxes for the drainages to the North Atlantic Ocean: natural and human influences. *Biogeochemistry* 35:75–139
Huyer A. 1983. Coastal upwelling in the California Current system. *Prog. Oceanogr.* 12:259–84
Irby ID, Friedrichs MAM, Da F, Hinson KE. 2018. The competing impacts of climate change and nutrient reductions on dissolved oxygen in Chesapeake Bay. *Biogeosciences* 15:2649–68

Irby ID, Friedrichs MAM, Friedrichs CT, Bever AJ, Hood RR, et al. 2016. Challenges associated with modeling low-oxygen waters in Chesapeake Bay: a multiple model comparison. *Biogeosciences* 13:2011–28

Izett JG, Fennel K. 2018a. Estimating the cross-shelf export of riverine materials: part 1. General relationships from an idealized numerical model. *Glob. Biogeochem. Cycles* 32:160–75

Izett JG, Fennel K. 2018b. Estimating the cross-shelf export of riverine materials: part 2. Estimates of global freshwater and nutrient export. *Glob. Biogeochem. Cycles* 32:176–86

Ji X, Sheng J, Tang L, Liu D, Yang X. 2011. Process study of circulation in the Pearl River Estuary and adjacent coastal waters in the wet season using a triply-nested circulation model. *Ocean Model.* 38:138–60

Johansson J. 2018. *Total and regional runoff to the Baltic Sea*. Baltic Sea Environ. Fact Sheet, HELCOM, Helsinki. **http://helcom.fi/baltic-sea-trends/environment-fact-sheets/hydrography/total-and-regional-runoff-to-the-baltic-sea**

Jonsson P, Carman R, Wulff F. 1990. Laminated sediments in the Baltic: a tool for evaluating nutrient mass balances. *Ambio* 19:152–58

Kemp WM, Boynton WR, Adolf JE, Boesch DF, Boicourt WC, et al. 2005. Eutrophication of Chesapeake Bay: historical trends and ecological interactions. *Mar. Ecol. Prog. Ser.* 303:1–29

Kemp WM, Sampou PA, Caffrey J, Mayer M, Henriksen K, Boynton WR. 1990. Ammonium recycling versus denitrification in Chesapeake Bay sediments. *Limnol. Oceanogr.* 35:1545–63

Kemp WM, Sampou PA, Garber J, Tuttle J, Boynton WR. 1992. Seasonal depletion of oxygen from bottom waters of Chesapeake Bay: roles of benthic and planktonic respiration and physical exchange processes. *Mar. Ecol. Prog. Ser.* 85:137–52

Laurent A, Fennel K. 2014. Simulated reduction of hypoxia in the northern Gulf of Mexico due to phosphorus limitation. *Elementa* 2:22

Laurent A, Fennel K. 2017. Modeling river-induced phosphorus limitation in the context of coastal hypoxia. In *Modeling Coastal Hypoxia: Numerical Simulations of Patterns, Controls and Effects of Dissolved Oxygen Dynamics*, ed. D Justic, KA Rose, RD Hetland, K Fennel, pp. 149–71. Cham, Switz.: Springer

Laurent A, Fennel K, Cai W-J, Huang W-J, Barbero L, Wanninkhof R. 2017. Eutrophication-induced acidification of coastal waters in the northern Gulf of Mexico: insights into origin and processes from a coupled physical-biogeochemical model. *Geophys. Res. Lett.* 44:946–56

Laurent A, Fennel K, Hu J, Hetland R. 2012. Simulating the effects of phosphorus limitation in the Mississippi and Atchafalaya River plumes. *Biogeosciences* 9:4707–23

Laurent A, Fennel K, Ko DS, Lehrter J. 2018. Climate change projected to exacerbate impacts of coastal eutrophication in the northern Gulf of Mexico. *J. Geophys. Res. Oceans* 123:3408–26

Laurent A, Fennel K, Wilson R, Lehrter J, Devereux R. 2016. Parameterization of biogeochemical sediment–water fluxes using in situ measurements and a diagenetic model. *Biogeosciences* 13:77–94

Lavik G, Stührmann T, Brüchert V, van der Plas A, Mohrholz V, et al. 2009. Detoxification of sulphidic African shelf waters by blooming chemolithotrophs. *Nature* 457:581–84

Lee M, Shevliakova E, Malyshev S, Milly PCD, Jaffé PR. 2016. Climate variability and extremes, interacting with nitrogen storage, amplify eutrophication risk. *Geophys. Res. Lett.* 43:7520–28

Lee YJ, Lwiza KMM. 2008. Characteristics of bottom dissolved oxygen in Long Island Sound, New York. *Estuar. Coast. Shelf Sci.* 76:187–200

Lehmann MF, Barnett B, Gélinas Y, Gilbert D, Maranger RJ, et al. 2009. Aerobic respiration and hypoxia in the Lower St. Lawrence Estuary: stable isotope ratios of dissolved oxygen constrain oxygen sink partitioning. *Limnol. Oceanogr.* 54:2157–69

Lehrter JC, Ko DS, Lowe LL, Penta B. 2017. Predicted effects of climate change on northern Gulf of Mexico hypoxia. In *Modeling Coastal Hypoxia: Numerical Simulations of Patterns, Controls and Effects of Dissolved Oxygen Dynamics*, ed. D Justic, KA Rose, RD Hetland, K Fennel, pp. 173–214. Cham, Switz.: Springer

Li M, Lee Y-J, Testa JM, Li Y, Ni W, et al. 2016. What drives interannual variability of estuarine hypoxia: climate forcing versus nutrient loading? *Geophys. Res. Lett.* 43:2127–34

Li Y, Li M, Kemp WM. 2015. A budget analysis of bottom-water dissolved oxygen in Chesapeake Bay. *Estuaries Coasts* 38:2132–48

Liu SM, Zhang J, Chen HT, Wu Y, Xiong H, Zhang ZF. 2003. Nutrients in the Changjiang and its tributaries. *Biogeochemistry* 62:1–18

Liu X, Zhang Y, Han W, Tang A, Shen J, et al. 2013. Enhanced nitrogen deposition over China. *Nature* 494:459–62

Ludwig W, Dumont E, Meybeck M, Heussner S. 2009. River discharges of water and nutrients to the Mediterranean and Black Sea: major drivers for ecosystem changes during past and future decades? *Prog. Oceanogr.* 80:199–217

Marta-Almeida M, Hetland RD, Zhang X. 2013. Evaluation of model nesting performance on the Texas-Louisiana continental shelf. *J. Geophys. Res. Oceans* 118:2476–91

Mattern JP, Fennel K, Dowd M. 2013. Sensitivity and uncertainty analysis of model hypoxia estimates for the Texas-Louisiana shelf. *J. Geophys. Res. Oceans* 118:1316–32

Matthäus W. 2006. *The history of investigation of salt water inflows into the Baltic Sea - from the early beginning to recent results*. Mar. Sci. Rep. 65, Baltic Sea Res. Inst., Rostock-Warnemünde, Ger.

Mee L. 2006. Reviving dead zones. *Sci. Am.* 295:78–85

Meier HEM, Hordoir R, Andersson HC, Dieterich C, Eilola K, et al. 2012. Modeling the combined impact of changing climate and changing nutrient loads on the Baltic Sea environment in an ensemble of transient simulations for 1961–2099. *Clim. Dyn.* 39:2421–41

Meier HEM, Väli G, Naumann M, Eilola K, Frauen C. 2018. Recently accelerated oxygen consumption rates amplify deoxygenation in the Baltic Sea. *J. Geophys. Res. Oceans* 123:3227–40

Mohrholz V, Bartholomae CH, van der Plas AK, Lass HU. 2008. The seasonal variability of the northern Benguela undercurrent and its relation to the oxygen budget on the shelf. *Cont. Shelf Res.* 28:424–41

Monteiro PMS, van der Plas AK, Melice J-L, Florenchie P. 2008. Interannual hypoxia variability in a coastal upwelling system: ocean–shelf exchange, climate and ecosystem-state implications. *Deep-Sea Res. I* 55:435–50

Monteiro PMS, van der Plas AK, Mohrholz V, Mabille E, Pascall A, Joubert W. 2006. Variability of natural hypoxia and methane in a coastal upwelling system: oceanic physics or shelf biology? *Geophys. Res. Lett.* 33:L16614

Moriarty JM, Harris CK, Friedrichs MAM, Fennel K, Xu K. 2018. Impact of seabed resuspension on oxygen and nitrogen dynamics in the northern Gulf of Mexico: a numerical modeling study. *J. Geophys. Res. Oceans* 123:7237–63

Murphy RR, Kemp WM, Ball WP. 2011. Long-term trends in Chesapeake Bay seasonal hypoxia, stratification, and nutrient loading. *Estuaries Coasts* 34:1293–309

Murrell MC, Stanley RS, Lehrter JC. 2013. Plankton community respiration, net ecosystem metabolism, and oxygen dynamics on the Louisiana continental shelf: implications for hypoxia. *Cont. Shelf Res.* 52:27–38

Natl. Park Serv. 2017. Mississippi River facts. *Natl. Park Serv.* **https://www.nps.gov/miss/riverfacts.htm**

Nausch G, Nehring D, Aertebjerg G. 1999. Anthropogenic nutrient load of the Baltic Sea. *Limnologica* 29:233–41

Neumann T, Fennel W, Kremp C. 2002. Experimental simulations with an ecosystem model of the Baltic Sea: a nutrient load reduction experiment. *Glob. Biogeochem. Cycles* 16:1033

Neumann T, Radtke H, Seifert T. 2017. On the importance of Major Baltic Inflows for oxygenation of the central Baltic Sea. *J. Geophys. Res. Oceans* 122:1090–101

Nixon SW. 1998. Enriching the sea to death. *Scientific American Presents*, Fall, pp. 48–53

Noffke A, Sommer S, Dale AW, Hall POJ, Pfannkuche O. 2016. Benthic nutrient fluxes in the Eastern Gotland Basin (Baltic Sea) with particular focus on microbial mat ecosystems. *J. Mar. Syst.* 158:1–12

O'Donnell J, Dam HG, Bohlen WF, Fitzgerald W, Gay PS, et al. 2008. Intermittent ventilation in the hypoxic zone of western Long Island Sound during the summer of 2004. *J. Geophys. Res. Oceans* 113:C09025

O'Shea ML, Brosnan TM. 2000. Trends in indicators of eutrophication in Western Long Island Sound and the Hudson-Raritan Estuary. *Estuaries* 23:877–901

Paerl HW, Valdes LM, Joyner AR, Piehler MF, Lebo ME. 2004. Solving problems resulting from solutions: evolution of a dual nutrient management strategy for the eutrophying Neuse River Estuary, North Carolina. *Environ. Sci. Technol.* 38:3068–73

Parker CA, O'Reilly JE. 1991. Oxygen depletion in Long Island Sound: a historical perspective. *Estuaries* 14:248–64

Pers C, Rahm L. 2000. Changes in apparent oxygen removal in the Baltic proper deep water. *J. Mar. Syst.* 25:421–29

Qian W, Dai M, Xu M, Kao S, Du C, et al. 2017. Non-local drivers of the summer hypoxia in the East China Sea off the Changjiang Estuary. *Estuar. Coast. Shelf Sci.* 198:393–99

Rabalais N, Turner R, Wiseman W Jr. 2002. Gulf of Mexico hypoxia, A.K.A. "the dead zone." *Annu. Rev. Ecol. Syst.* 33:235–63

Rabouille C, Conley DJ, Dai MH, Cai W-J, Chen CTA, et al. 2008. Comparison of hypoxia among four river-dominated ocean margins: the Changjiang (Yangtze), Mississippi, Pearl, and Rhône rivers. *Cont. Shelf Res.* 28:1527–37

Sale JW, Skinner WW. 1917. The vertical distribution of dissolved oxygen and the precipitation by salt water in certain tidal areas. *J. Frankl. Inst.* 184:837–48

Saucier FJ, Chasse J. 2000. Tidal circulation and buoyancy effects in the St. Lawrence Estuary. *Atmos.-Ocean* 38:505–56

Saucier FJ, Roy F, Gilbert D, Pellerin P, Ritchie H. 2003. Modeling the formation and circulation processes of water masses and sea ice in the Gulf of St. Lawrence, Canada. *J. Geophys. Res. Oceans* 108:3269

Schmidt M, Eggert A. 2016. Oxygen cycling in the northern Benguela Upwelling System: modelling oxygen sources and sinks. *Prog. Oceanogr.* 149:145–73

Scully ME. 2010. Wind modulation of dissolved oxygen in Chesapeake Bay. *Estuaries Coasts* 33:1164–75

Scully ME. 2013. Physical controls on hypoxia in Chesapeake Bay: a numerical modeling study. *J. Geophys. Res. Oceans* 118:1239–56

Scully ME. 2016. The contribution of physical processes to inter-annual variations of hypoxia in Chesapeake Bay: a 30-yr modeling study. *Limnol. Oceanogr.* 61:2243–60

Seitzinger SP, Mayorga E, Bouwman AF, Kroeze C, Beusen AHW, et al. 2010. Global river nutrient export: a scenario analysis of past and future trends. *Glob. Biogeochem. Cycles* 24:GB0A08

Sharples J, Middelburg JJ, Fennel K, Jickells TD. 2017. What proportion of riverine nutrients reaches the open ocean? *Glob. Biogeochem. Cycles* 31:39–58

Siedlecki SA, Banas NS, Davis KA, Giddings S, Hickey BM, et al. 2015. Seasonal and interannual oxygen variability on the Washington and Oregon continental shelves. *J. Geophys. Res. Oceans* 120:608–33

Sinha E, Michalak AM, Balaji V. 2017. Eutrophication will increase during the 21st century as a result of precipitation changes. *Science* 357:405–8

Slomp CP, Van Cappellen P. 2007. The global marine phosphorus cycle: sensitivity to oceanic circulation. *Biogeosciences* 4:155–71

Smith EM, Kemp WM. 1995. Seasonal and regional variations in plankton community production and respiration for Chesapeake Bay. *Mar. Ecol. Prog. Ser.* 116:217–31

Sylvan JB, Dortch Q, Nelson DM, Maier Brown AF, Morrison W, Ammerman JW. 2006. P limits phytoplankton growth on the Louisiana shelf during the period of hypoxia formation. *Environ. Sci. Technol.* 40:7548–53

Sylvan JB, Quigg A, Tozzi S, Ammerman J. 2007. Eutrophication-induced phosphorus limitation in the Mississippi River plume: evidence from fast repetition rate fluorometry. *Limnol. Oceanogr.* 52:2679–85,

Testa JM, Clark JB, Dennison WC, Donovan EC, Fisher AW, et al. 2017. Ecological forecasting and the science of hypoxia in Chesapeake Bay. *BioScience* 67:614–26

Testa JM, Kemp WM. 2011. Oxygen – dynamics and biogeochemical consequences. In *Treatise on Estuarine and Coastal Science*, Vol. 5, ed. E Wolanski, DS McLusky, pp. 163–99, Waltham, MA: Academic

Testa JM, Kemp WM. 2014. Spatial and temporal patterns in winter-spring oxygen depletion in Chesapeake Bay bottom waters. *Estuaries Coasts* 37:1432–48

Testa JM, Li Y, Lee YJ, Li M, Brady DC, et al. 2014. Quantifying the effects of nutrient loading on dissolved O_2 cycling and hypoxia in Chesapeake Bay using a coupled hydrodynamic-biogeochemical model. *J. Mar. Syst.* 139:139–58

Testa JM, Murphy RR, Brady DC, Kemp WM. 2018. Nutrient- and climate-induced shifts in the phenology of linked biogeochemical cycles in a temperate estuary. *Front. Mar. Sci.* 5:114

Turner RE, Rabalais NN. 1991. Changes in Mississippi River water quality this century. *BioScience* 41:140–47

US Environ. Prot. Agency. 2017. *Hypoxia in Gulf of Mexico and Long Island Sound*. Rep. Environ., US Environ. Prot. Agency, Washington, DC. **https://cfpub.epa.gov/roe/indicator_pdf.cfm?i=41**

Vaquer-Sunyer R, Duarte C. 2008. Thresholds of hypoxia for marine biodiversity. *PNAS* 105:15452–57

Vieira MEC. 2000. The long-term residual circulation in Long Island Sound. *Estuaries Coasts* 23:199–207
Wang B. 2009. Hydromorphological mechanisms leading to hypoxia off the Changjiang estuary. *Mar. Environ. Res.* 67:53–58
Wang B, Wei Q, Chen J, Xie L. 2012. Annual cycle of hypoxia off the Changjiang (Yangtze River) Estuary. *Mar. Environ. Res.* 77:1–5
Wang J, Yan W, Chen N, L X, Liu L. 2015. Modeled long-term changes of DIN:DIP ratio in the Changjiang River in relation to Chl-α and DO concentrations in adjacent estuary. *Estuar. Coast. Shelf Sci.* 166:153–60
Welsh BL, Eller FC. 1991. Mechanisms controlling summertime oxygen depletion in western Long Island Sound. *Estuaries* 14:265–78
Wilson RE. 1976. Gravitational circulation in Long Island Sound. *Estuar. Coast. Mar. Sci.* 4:443–53
Wilson RE, Bratton SD, Wang J, Colle BA. 2015. Evidence for directional wind response in controlling interannual variations in duration and areal extent of summertime hypoxia in western Long Island Sound. *Estuaries Coasts* 38:1735–43
Wilson RE, Swanson RL, Crowley HA. 2008. Perspectives on long-term variations in hypoxia conditions in western Long Island Sound. *J. Geophys. Res. Oceans* 113:C12011
Wiseman W, Rabalais N, Turner R, Dinnel S, Mac-Naughton A. 1997. Seasonal and interannual variability within the Louisiana coastal current: stratification and hypoxia. *J. Mar. Syst.* 12:237–48
Wolfe DA, Monahan R, Stacey PE, Farrow DRG, Robertson A. 1991. Environmental quality of Long Island Sound: assessment and management issues. *Estuaries* 14:224–36
Wong GTF, Gong G, Liu K, Pai S. 1998. 'Excess nitrate' in the East China Sea. *Estuar. Coast. Shelf Sci.* 46:411–18
Wulff F, Humborg C, Andersen HE, Blicher-Mathiesen G, Czajkowski M, et al. 2014. Reduction of Baltic Sea nutrient inputs and allocation of abatement costs within the Baltic Sea Catchment. *Ambio* 43:11
Wulff F, Stigebrandt A. 1989. A timed-dependent budget model for nutrients in the Baltic Sea. *Glob. Biogeochem. Cycles* 3:63–78
Yan W, Zhang S, Sun P, Seitzinger SP. 2003. How do nitrogen inputs to the Changjiang basin impact the Changjiang River nitrate: a temporal analysis for 1968–1997. *Glob. Biogeochem. Cycles* 17:1091
Yang D, Yin B, Liu Z, Bai T, Qi J, Chen H. 2012. Numerical study on the pattern and origins of Kuroshio branches in the bottom water of southern East China Sea in summer. *J. Geophys. Res. Oceans* 117:C02014
Yang D, Yin B, Liu Z, Feng X. 2011. Numerical study of the ocean circulation on the East China Sea shelf and a Kuroshio bottom branch northeast of Taiwan in summer. *J. Geophys. Res. Oceans* 116:C05015
Yin KD, Lin ZF, Ke ZY. 2004. Temporal and spatial distribution of dissolved oxygen in the Pearl River Estuary and adjacent coastal waters. *Cont. Shelf Res.* 24:1935–48
Yu L, Fennel K, Laurent A. 2015a. A modeling study of physical controls on hypoxia generation in the northern Gulf of Mexico. *J. Geophys. Res. Oceans* 120:5019–39
Yu L, Fennel K, Laurent A, Murrell MC, Lehrter JC. 2015b. Numerical analysis of the primary processes controlling oxygen dynamics on the Louisiana shelf. *Biogeosciences* 12:2063–76
Zhang H, Li S. 2010. Effects of physical and biochemical processes on the dissolved oxygen budget for the Pearl River Estuary during summer. *J. Mar. Syst.* 79:65–88
Zhang H, Zhao L, Sun Y, Wang J, Wei H. 2017. Contribution of sediment oxygen demand to hypoxia development off the Changjiang Estuary. *Estuar. Coast. Shelf Sci.* 192:149–57
Zhang Q, Brady DC, Boynton WR, Ball WP. 2015. Long-term trends of nutrients and sediment from the nontidal Chesapeake watershed: an assessment of progress by river and season. *J. Am. Water Resour. Assoc.* 51:1534–55
Zhang W, Hetland RD, DiMarco SF, Fennel K. 2015. Processes controlling mid-water column oxygen minima over the Texas-Louisiana Shelf. *J. Geophys. Res. Oceans* 120:2800–12
Zhao L, Guo X. 2011. Influence of cross-shelf water transport on nutrients and phytoplankton in the East China Sea: a model study. *Ocean Sci.* 7:27–43
Zhou F, Chai F, Huang D, Xue H, Chen J, et al. 2017. Investigation of hypoxia off the Changjiang Estuary using a coupled model of ROMS-CoSiNE. *Prog. Oceanogr.* 159:237–54

Zhu Z-Y, Wu H, Liu S-M, Wu Y, Huang D-J, et al. 2017. Hypoxia off the Changjiang (Yangtze River) estuary and in the adjacent East China Sea: quantitative approaches to estimating the tidal impact, and nutrient regeneration. *Mar. Pollut. Bull.* 125:103–14

Zhu Z-Y, Zhang J, Wu Y, Zhang Y-Y, Lin J, Liu S-M. 2011. Hypoxia off the Changjiang (Yangtze River) Estuary: oxygen depletion and organic matter decomposition. *Mar. Chem*. 125:108–16

Zillén L, Conley DJ, Andren T, Andren E, Gjorck S. 2008. Past occurrences of hypoxia in the Baltic Sea and the role of climate variability, environmental change and human impact. *Earth Sci. Rev.* 91:77–92

Zimmerman AR, Canuel EA. 2000. A geochemical record of eutrophication and anoxia in Chesapeake Bay sediments: anthropogenic influence on organic matter composition. *Mar. Chem*. 69:117–37

Annual Review
of Marine Science

Volume 11, 2019

Contents

Passing the Baton to the Next Generation: A Few Problems That Need Solving
Cindy Lee 1

A Conversation with Walter Munk
Walter Munk and Carl Wunsch 15

Compound-Specific Isotope Geochemistry in the Ocean
Hilary G. Close 27

Mechanisms and Pathways of Small-Phytoplankton Export from the Surface Ocean
Tammi L. Richardson 57

Using Noble Gases to Assess the Ocean's Carbon Pumps
Roberta C. Hamme, David P. Nicholson, William J. Jenkins, and Steven R. Emerson 75

Biogeochemical Controls on Coastal Hypoxia
Katja Fennel and Jeremy M. Testa 105

Planktonic Marine Archaea
Alyson E. Santoro, R. Alexander Richter, and Christopher L. Dupont 131

The Variable Southern Ocean Carbon Sink
Nicolas Gruber, Peter Landschützer, and Nicole S. Lovenduski 159

Arctic and Antarctic Sea Ice Change: Contrasts, Commonalities, and Causes
Ted Maksym 187

Biologically Generated Mixing in the Ocean
Eric Kunze 215

Global Air–Sea Fluxes of Heat, Fresh Water, and Momentum: Energy Budget Closure and Unanswered Questions
Lisan Yu 227

The Global Overturning Circulation
Paola Cessi 249

The Water Mass Transformation Framework for Ocean Physics and Biogeochemistry
Sjoerd Groeskamp, Stephen M. Griffies, Daniele Iudicone, Robert Marsh, A.J. George Nurser, and Jan D. Zika 271

Climate Change, Coral Loss, and the Curious Case of the Parrotfish Paradigm: Why Don't Marine Protected Areas Improve Reef Resilience?
John F. Bruno, Isabelle M. Côté, and Lauren T. Toth 307

Marine Environmental Epigenetics
Jose M. Eirin-Lopez and Hollie M. Putnam 335

Marine Metazoan Modern Mass Extinction: Improving Predictions by Integrating Fossil, Modern, and Physiological Data
Piero Calosi, Hollie M. Putnam, Richard J. Twitchett, and Fanny Vermandele 369

Partnering with Fishing Fleets to Monitor Ocean Conditions
Glen Gawarkiewicz and Anna Malek Mercer 391

The Scientific Legacy of the CARIACO Ocean Time-Series Program
Frank E. Muller-Karger, Yrene M. Astor, Claudia R. Benitez-Nelson, Kristen N. Buck, Kent A. Fanning, Laura Lorenzoni, Enrique Montes, Digna T. Rueda-Roa, Mary I. Scranton, Eric Tappa, Gordon T. Taylor, Robert C. Thunell, Luis Troccoli, and Ramon Varela 413

Unoccupied Aircraft Systems in Marine Science and Conservation
David W. Johnston 439

Windows into Microbial Seascapes: Advances in Nanoscale Imaging and Application to Marine Sciences
Gordon T. Taylor 465

The Formation and Distribution of Modern Ooids on Great Bahama Bank
Paul (Mitch) Harris, Mara R. Diaz, and Gregor P. Eberli 491

Errata

An online log of corrections to *Annual Review of Marine Science* articles may be found at http://www.annualreviews.org/errata/marine